



Creep and Collapse Behaviour of Mechanically and Biologically Pre-treated Solid Waste in Oedometer Tests

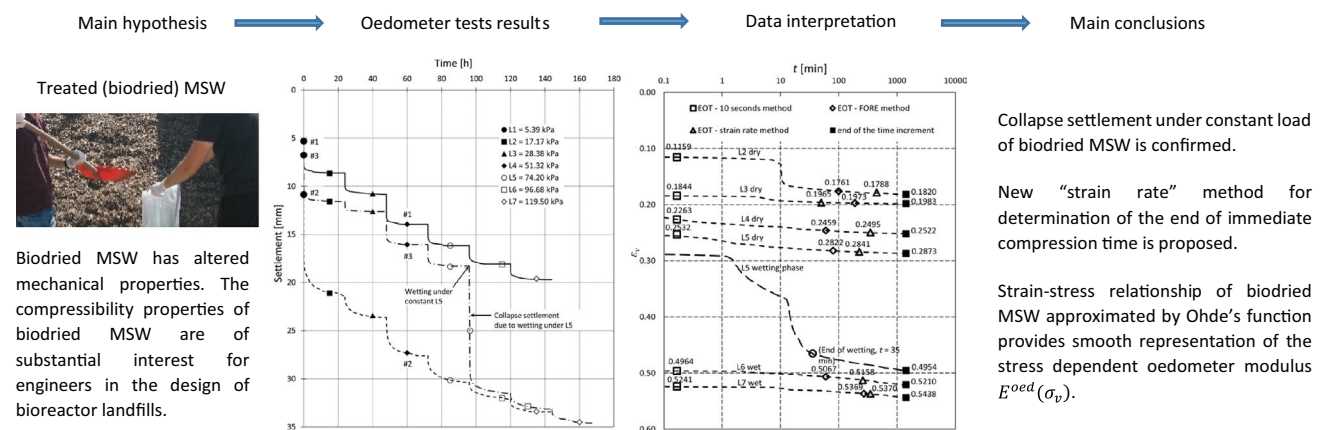
Nikola Kaniški¹ · Nikola Hrnčić¹ · Igor Petrović¹ · Erich Bauer²

Received: 28 October 2022 / Accepted: 11 February 2023
© The Author(s), under exclusive licence to Springer Nature B.V. 2023

Abstract

The paper deals with the compression behaviour of mixed fractions of a mechanically treated and biologically dried waste material with methanogenic fraction appropriate for landfilling in a bioreactor landfill. To this end oedometric compression tests were carried out with specimens taken from the Waste Management Center Marišćina, in Croatia. The compression behaviour up to a maximum vertical stress of 119.5 kPa was investigated in a sequence of seven load steps with an adapted oedometer device under three different drained test conditions: the dry state, the wet state, and wetting of the initially dry and pre-compressed material. The interpretation of experimental data focuses on the immediate compression and mechanical creep behaviour obtained within each load step. As the settlements are time dependent from the beginning of loading, no clear distinction between immediate and secondary compression can be gathered from the settlement-time curves. To this end a fictitious time where the immediate settlement ends is introduced based on common methods and a new method proposed in this paper. The latter, is named the strain-rate method, which defines the time where a given strain rate is relevant for the transition from the immediate compression to mechanical creep. Within the stress range considered, the approximation of mechanical creep using the so-called modified secondary compression index showed that the value of this index decreases for the moist waste material but it is almost constant for the dry material. Particular attention is also paid to so-called collapse settlements under constant load which can take place as a result of an increase of the moisture content. For the mathematical description of the mechanical behaviour enhanced approximation functions are proposed, which are also easy to handle for practical application. The experimental results are comprehensively discussed and compared with data from the literature.

Graphical Abstract



Keywords MBT waste · Biodried methanogenic fraction · Oedometric compression · Immediate compression · Mechanical creep · Wetting-induced collapsibility

Extended author information available on the last page of the article

Statement of Novelty

A reformulated compression law by Ohde which permits a closer approximation of the oedometer experimental data than the modified compression index is proposed. The paper also considers a more detailed discussion of the distinction between immediate and secondary compression. Apart from some common methods such as the “FORE method” a new method with the name “Strain-rate method” was proposed, which assumes a fictitious strain rate where immediate compression turns into mechanical creep. In addition, the so-called collapsibility behaviour caused by wetting of the initially pre-compressed material under dry condition was also investigated. It is argued that the mechanisms of collapse settlements are most probably due to softening of hydrophilic waste particles and particle contacts caused by wetting.

Introduction

As a response to the requirements of the Waste Framework Directive (2008/98/EC) [1] to prevent or, at least, to reduce the unfavourable impact on the environment and human health caused by untreated landfills, many European countries have developed and implemented various procedures for the mechanical and biological treatment (MBT) of municipal solid waste (MSW). The most common, and widely adopted MBT process, is the composting or so-called biostabilisation process. In the biostabilising MBT plant the main goal is to obtain inert waste stream without tendencies to any further meaningful physical, biological or chemical changes. In the MBT plant, which utilizes biostabilisation, the MSW is first mechanically treated and sorted. The rest of the material is then submitted to the biostabilisation process until all of its organic components are decomposed. The final product after biostabilisation has to be landfilled. A completely different process to the biostabilisation process, and one that has drawn increasing attention in the past decade, is the so-called biodrying process. In the MBT plant, which utilizes biodrying, the waste material is first submitted to the biodrying process and then mechanically treated and sorted in several waste streams. One of the final waste-streams that is obtained from the biodrying process is the so-called methanogenic fraction. In contrast to the biostabilisation process, the remained portion of organic components in the methanogenic fraction is still significant, and therefore still biologically active. This makes methanogenic fraction suitable for landfilling in what is known as bioreactor landfill. After mechanical and biological treatment,

municipal solid waste has altered mechanical properties. The compressibility of mechanically treated and biologically dried waste material with a methanogenic fraction can be accompanied by collapse effects and time dependent properties which strongly depend on the change of the moisture content and the technology used for pre-treatment of the material.

The mechanical properties of biodried methanogenic fraction are of substantial interest for engineers in the design and the safety issues of bioreactor landfills. While many researchers have investigated the compression behaviour of raw municipal solid waste material [2–22], their result cannot be directly related to MBT waste materials, because MBT process significantly alters the mechanical properties of MSW.

Many researchers were also involved in the testing of biostabilised MBT waste. The earliest pioneering work was largely done by researchers in Austria, Germany and Italy, e.g. [23–28]. In the past decade scientific interest in the compression behaviour of biostabilised MBT waste has become more widespread, e.g. [29–36]. Petrovic et al. [34] studied the compressibility of biostabilised MBT waste using a large scale oedometer with a specimen diameter of 500 mm. Under a pressure of 400 kPa, a compaction between 20–30% was observed. The comparison of the virgin compression curve with the unloading curve indicates that only a minor part of the total deformation can be recovered. Thus, the main deformation of the waste material is inelastic. The obtained stiffness module fitted well within the range of the stiffness module obtained for waste materials of similar characteristics by other authors [23, 24, 37, 38]. Moreover, in the experiment by Petrovic et al. [34] the stiffness module obtained with biostabilised MBT waste were also compared with the stiffness module of raw waste material published by Jesberger and Kockel [2]. It was found that the biostabilisation of waste material prior to landfilling shows similar stiffness properties to the raw waste material, which was landfilled over a decade. The short-term compression-rebound and long-term compression tests carried out by Zhang et al. [36] showed that the immediate compression ratio ranged between 0.233 and 0.247, which was comparable to the aged high food waste content. The mechanical creep ratio ranged between 0.012 and 0.018, being close to the fresh and aged MSWs. In contrast to the situation for biostabilised waste, data about the compression behaviour of biodried waste materials with a methanogenic fraction are rare. While many researchers were interested in optimizing the biodrying process [39–46], the mechanical behaviour of biodried waste material with methanogenic fraction is barely investigated.

A question of specific interest is the mechanisms behind collapse settlements caused by wetting of an initially dry material. Experiments show that the classical effective stress

theory originally introduced by Terzaghi [47] for granular materials with incompressible particles fails for fully saturated waste materials with a portion of compressible particles, e.g. Shariatmadari et al. [48]. In order to take into account the compressibility of particles in the effective stress relation, various theories are proposed in the literature, e.g. Biot [49], Skempton [50], de Boer [51], Ehlers [52], Zhang et al. [53], Powrie et al. [54], Liang et al. [55]. Whether enhanced effective stress concepts are appropriate for explaining the mechanisms of collapse settlements, however, it is still an open question. A closer inspection of the literature indicates that the mechanism of wetting induced collapse settlement of waste, e.g. Sowers [56], is in a phenomenological manner similar to that as observed in weathered and moisture sensitive coarse-grained rockfills, where wetting settlements cannot be explained by the concept of effective stresses (Brauns et al. [57]; Bauer [58]; Ham et al. [59]). The mechanism of wetting settlements is mainly related to the moisture dependent degradation of the particle hardness (Bauer et al. [60]). For partly or fully saturated waste materials composed of a mixture of various non-organic and organic matter, the individual properties of particles, i.e. the moisture and pressure dependent degradation of particle strength, the porosity, the water adsorption characteristic, the contact behaviour between particles of different materials, the suction and the coupled mechanical behaviour of particle assemblies is still a challenging task for a comprehensive experimental investigation and also for the calibration of refined constitutive models.

In this paper, the focus is on the one dimensional compressibility and collapsibility of the dry and wet state of mechanically treated and biologically dried waste material with a methanogenic fraction. The pre-treated waste material for the experiments was taken from the MBT plant Marišćina, Istria, in Croatia and consists of a mixture of shredded particles including the following main components: plastic, paper, textiles, glass, metal, wood, stones, ceramics and kitchen waste. The adapted oedometer equipment that was used permits the study of various scenarios, which can occur within the bioreactor landfill body. These are the compression behaviour of the waste material under the following conditions: dry state, wet state, pre-loading under dry state and wetting under constant vertical load. For these three particular states the time-dependent compression behaviour of the material was investigated under drained conditions for a total test duration of approx. 145 h and a maximum vertical stress of 119.5 kPa, which was applied in a sequence of seven load steps. The considered stress range is also relevant to that for landfilling at the Waste Management Center Marišćina, in Croatia. In order to avoid biodegradation of organic matter during the experiment, wetting was carried out with a mixture of acetic and propionic acid dissolved in deaerated water. The settlements caused by

degradation process were thus not taken into account in the present research. For the interpretation of the time dependent evolution of the load settlement data, particular attention was paid on the distinction between immediate and secondary compression. To this end the conceptual settlement model proposed by Bareither et al. [61] is considered, which, in general, distinguishes four time-dependent transition phases under constant stress, i.e. immediate compression, mechanical creep, bio-compression and final mechanical creep. Since the long-term creep behaviour influenced by biodegradation was not investigated experimentally in the present research, this paper has as its subjects only immediate compression and mechanical creep. The results of all experiments are represented in total stresses measured on the boundary of the waste specimens.

As no clear distinction between immediate settlements and mechanical creep can be gathered from the settlement-time curves the assumption of a fictitious time is required to define the end of the immediate settlement (EOT). Various pragmatic concepts for the estimation of the fictitious time are proposed in the literature, e.g. [7, 62–66]. For instance, Rakic et al. [66] assumed a fixed EOT value of 15 min, while Bareither et al. [7] proposed for the determination of the EOT value a combination of the so-called “FORE Method”, originally presented by Handy [67], with the assumption that the section of mechanical creep can be described in the semi-logarithmic representation using a constant mechanical creep ratio. Thus, for the time dependent compression under constant stress the EOT value is defined for the state in which the compression curve in a semi-logarithmic representation turns into a straight line. In order to overcome the influence of the scattering of experimental data a so-called “modified FORE method” is also applied where a smoothed representation of the experimental data is used in contrast to the original “FORE method”. To estimate the EOT value for the time dependent compression curves obtained in the present research common methods, i.e. the “10 s method”, the “FORE method”, the “Modified FORE method” are applied and compared with the so-called “Strain-rate method”. The latter is an alternative new method proposed in this paper. The strain-rate method assumes a fictitious strain rate where immediate compression turns into mechanical creep. In contrast to other methods the “Strain-rate method” is directly related to an intrinsic material property under creep and thus allows an easy determination of EOT values for a series of experiments for a predefined strain rate.

The paper is organized as follows. In “[Components of the oedometer device](#)” the components of the oedometer device used in experiments are presented. “[Physical characteristics of the biodried MBT waste material](#)” summarizes the physical parameters of the waste material used in the experiments. The installation of the specimen and test procedure are outlined in “[Testing procedure](#)”. In “[Experimental results of](#)

"short-term oedometer compression tests" the experimental results, i.e. the mechanical parameter for immediate compression and mechanical creep are presented and compared with the data published by other researchers. Conclusions are summarized in "Conclusions".

Components of the Oedometer Device

As illustrated in Fig. 1 the used oedometer device consists of a compression cell, loading system and monitoring system. The cylindrical compression cell is made of stainless steel. The specimen ring has an inner diameter of 150 mm and can hold specimens up to 80 mm. The top plate is graded and guided by an upper ring to reduce side wall friction. In addition, the lateral surface of the top plate was sprinkled with talc powder before installing the specimen. The self-weight

of the top plate acts on the specimen with a vertical stress of 5.39 kPa. The top plate has a threaded hole at the top, on which a four-part steel rod with the overall length of 275 mm can be mounted. The rod operates as a guide in order to ensure that the applied dead load is in the centre of the compression cell. The rod yields an additional vertical stress of 2 kPa to the specimen. For the dead load a 30 mm thick square metal plates with a side length of 295 mm were used. Each plate can provide a vertical stress of 11.21 kPa to the specimen. In the centre of the plates a hole with a diameter of 50 mm keeps the applied load in the axis of the compression cell. The metal plates are placed on the specimen with help of a crane and an Archimedean pulley.

Figure 2 shows the oedometer assembly together with the measuring system installed in the laboratory. In particular, the compression cell is conveniently positioned on the already existing platform of the larger oedometer

Fig. 1 Illustration of the oedometer device cross-section

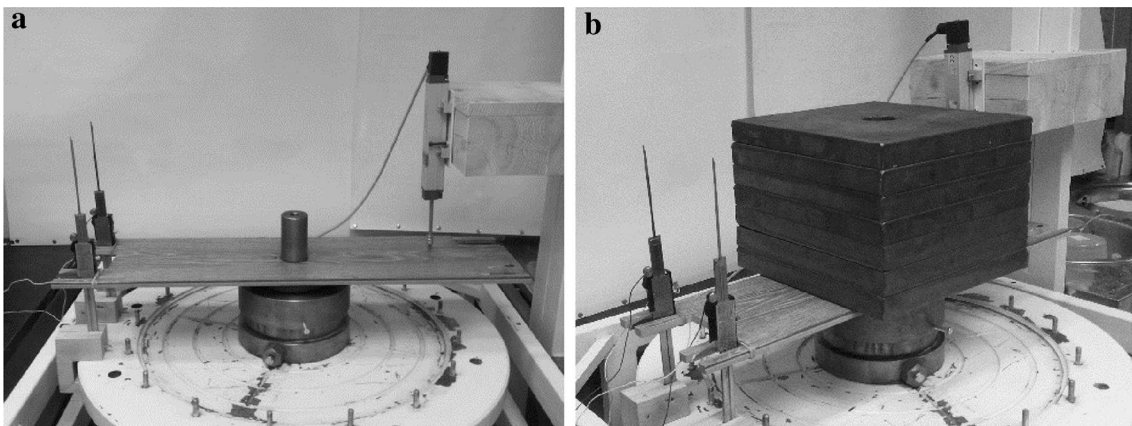
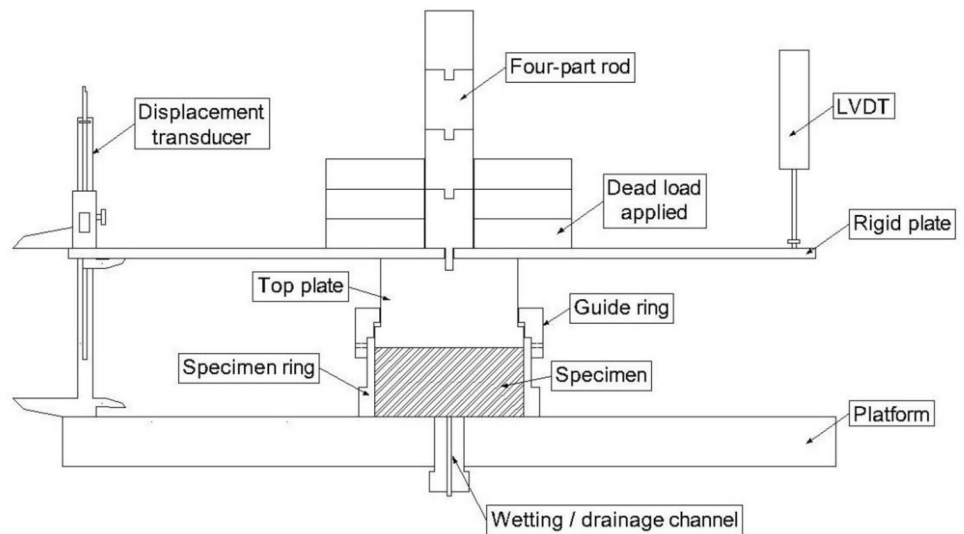


Fig. 2 Oedometer assembly placed on a large platform with incised channels: **a** compression cell without dead loads; **b** compression cell with applied dead loads

device developed by Petrovic et al. [34]. In the centre of the base plate the vertical channel works as wetting/saturating channel to inject fluid into the initially dry or moist specimen, as well as the drainage path for the excess pore water of wet specimens during consolidation.

In order to secure uniform settlement of the cylindrical specimen, a possible tilting of the top plate is reduced with the help of the guiding ring placed on the specimen ring. In order to exclude experiments with significant tilting of the top plate, which can be effected by a pronounced inhomogeneous specimen, the vertical displacement of the surface of the top plate during loading is checked with three displacement transducers. As a means of gaining a more precise measure of tilting the displacement transducers are placed at the end of a rigid plate, which is connected with the top plate of the compression cell as shown in Fig. 2. The three displacement transducers are positioned in a triangular shape, so that a tilting occurrence of the top plate can be determined from the measured settlement differences. Two displacement transducers with a resolution of 0.01 mm were placed on the left hand side. These displacement transducers were connected to the computer via the Arduino platform and the displacements were logged every second. The third transducer, i.e. a Vishay 115 L linear transducer with a resolution of 0.1 mm was placed on the right hand side and connected to the computer through an independent data logger. The displacements were recorded every ten seconds.

Physical Characteristics of the Biodried MBT Waste Material

In the experiments mechanically shredded and biologically dried waste material with a methanogenic fraction was taken from the MBT plant Marišćina, in Istria, Croatia. A brief summary of the procedure for the pre-treatment of the waste material carried out in the MBT plant is outlined by Petrovic et al. [68].

Composition of the MBT Waste Material

Two representative specimens of 1 kg each were taken by quartering method from the 30 kg sampled MBT waste. The applied procedure was adopted from ASTM D6323-19 [69] standard. In order to determine the composition of the waste material the individual ingredients were manually separated and weighed. The components and corresponding mean values of the mass portion from the specimens are summarized in Table 1. The parts of the waste here that could neither be identified nor separated are declared as “Unidentified”.

Table 1 Mass portion of MBT waste components

Component	Mass portion [%]
Plastics	6.43
Textile	0.22
Glass	10.62
Metal	0.94
Paper/cardboard	4.71
Wood	1.18
Bones/skin	0.20
Stones	2.76
Ceramics	0.46
Rubber	0.13
Kitchen waste	2.15
Unidentified > 2 mm	42.48
Unidentified < 2 mm	27.72
Total	100

Particle Size Distribution

The procedure for particle size analysis was adopted from ASTM D 422 [70] standard for Particle-Size Analysis of Soils. A total of 25 specimens were sieved on a series of sieves with hole sizes of: 31.5, 16, 8, 4, 2, 1 and 0.5 mm. The particle size distribution averaged from all specimens is shown in Fig. 3 and has a mean particle diameter of approximately 6 mm which is 25 times larger than the diameter of the oedometer specimen. More than 90% of particles were smaller than 25 mm. A minor proportion only were in the larger range between 31.5 mm and 50 mm and these were soft particles such as paper or plastic strips manufactured by the process of shredding.

Although a biodried MBT waste material was used in the present study, the corresponding particle size distribution curve lies rather well within the range of the particle size distribution curves obtained with biostabilised MBT waste materials from Austria, Germany and UK as also shown in Fig. 3.

Organic Matter

The procedure followed for the determination of the organic matter content was in accordance with the ASTM D 2974 [71] standard for measuring moisture, ash, and organic matter of peat and other organic soils. To this end a specimen with the mass of 50.04 g was used in which the mass portion of the individual components have a fair correspondence with the mass portion of waste components presented in Table 1. Each individual component was tested separately. To this end each component was placed in an own container and then subjected to the ignition process in the muffle furnace under 440°C until no further changes in mass were

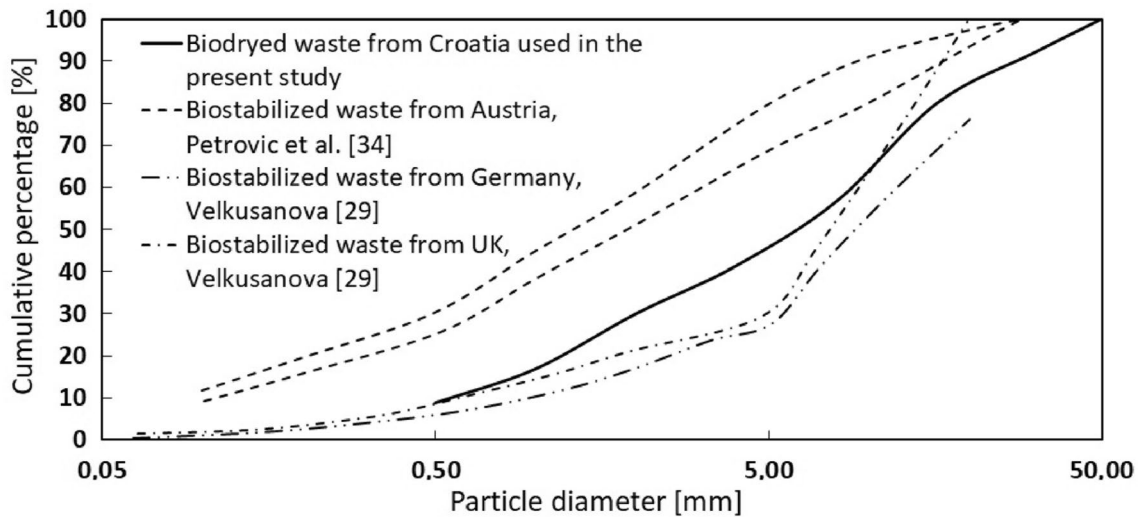


Fig. 3 Particle size distribution curves of the tested material and other publications

Table 2 Biodegradable content

Component	Mass [g]	Mass loss caused by ignition process [g]	Organic mass portion on the basis of the total mass [%]
Plastics	3.29	2.411	4.81
Textile	0.14	0.103	0.21
Glass	5.32	0.007	0.01
Metal	0.33	0.091	0.18
Paper/cardboard	2.44	1.929	3.86
Wood	0.60	0.538	1.07
Bones/skin	0.09	0.036	0.07
Stones	1.51	0.016	0.03
Ceramics	0.26	0.028	0.05
Rubber	0.05	0.021	0.04
Kitchen waste	1.19	0.944	1.89
Unidentified > 2 mm	21.00	14.00	27.98
Unidentified < 2 mm	13.82	5.711	11.41
Total	50.04	25.83	51.62

observed. Based on the differences of the weight before and after the ignition process, the mass portion of the organic content of each individual component were determined. Table 2 shows the organic content of each individual component which reveals that the total quantity of organic content in the examined specimen is 51.62%.

Particle Density

The particle density of MBT waste mixture was determined using a modified gas pycnometer. The gas pycnometer method is adapted from the ASTM D 5550 [72] standard. The results obtained from 5 specimens vary from 1.811 g/cm³ to 1.998 g/cm³. The scattering of the data is caused by a certain variation in size of individual waste particles and

strong inhomogeneity of tested specimens (Yesiller et al. [73]). The average value obtained from the 5 specimens is 1.894 g/cm³.

Testing Procedure

Three specimens, in the following, denoted as #1, #2 and #3, were placed into the oedometer cell as shown in Fig. 4. Prior installation the MBT waste material was subjected to an oven temperature of 60⁰ C for 24 h. All specimens had a mass of 0.4224 kg, an average solid density of $\rho_s = 1.894$ g/cm³, and thus, the volume of the solid material can be calculated to 223.0 cm³. The material was installed in three consecutive layers. In order to achieve a dry density of



Fig. 4 Dry specimen installed in the oedometer cell and weight used for initial compaction

approximately 0.38 g/cm^3 , which is relevant at the landfill location in Marišćina, each layer was compressed with help of weight of 2 kg (Fig. 4).

To support a homogeneous drainage of the specimen during loading a geotextile layer was placed at the bottom of the cell. On the top of the specimen, a geomembrane was placed to prevent fines of the specimen to enter the small gap between the oedometer ring and the top plate.

The three tested specimens were loaded in seven load steps L1 to L7 under different test conditions. In order to compare the influence of dry and wet state of the specimens on the compression behaviour, all three specimens were loaded in steps with the same sequence of load increments, i.e. the accumulated vertical stresses were for L1 = 5.39 kPa, L2 = 17.17 kPa, L3 = 28.38 kPa, L4 = 51.32 kPa, L5 = 74.2 kPa, L6 = 96.68 kPa and L7 = 119.5 kPa. The first vertical stress of 5.39 kPa results from the weight of the top platen. Immediately after reading the corresponding initial settlement under L1, an additional load plate acting with a vertical stress of 11.78 kPa on the specimen was applied. Thus, in the second load step L2 the vertical stress is $5.39 + 11.78 = 17.17 \text{ kPa}$. To investigate also the evolution of creep settlements the load was kept constant for 24 h before the next load increment was applied. Similar procedure was also applied for the subsequent load steps L2 to L7.

Table 3 Physical parameters of tested specimens in the initial state

Specimen	ρ [g/cm^3]	w [%]	ρ_d [g/cm^3]	ρ_s [g/cm^3]	e_0	S_r [%]
#1	0.38 *	0	0.38	1.894	3.984	0
#2	0.8588**	126.9	0.3785	1.894	4.005	60.02
#3	0.3758 *	0	0.3758	1.894	4.04	0

*Dry state

**Wet state

The applied maximum vertical stress of $L7 = 119.5 \text{ kPa}$ is a little more than the vertical stress of 80 kPa estimated at the bottom of the 21 m high Mariscina landfill.

Specimen #1 with an initial height of 62.9 mm was compressed under dry condition. Specimen #2 was wetted with a solution of deaerated water mixed with 10 g acetic acid and 10 g propionic acid per litre of fluid. The addition of acetic acid and propionic acid should prevent biodegradation process during the test (Siddiqui et al. [31]). The liquid was added slowly enough to prevent any disturbances of the installed specimen. In particular, with an Enterprise Level Pressure Volume Controller a total volume of 535.974 cm^3 of the liquid was added. The solution was added to the specimen from the bottom of the oedometer cell. Before loading specimen #2 had an initial height of 63.15 mm. Specimen #3 was first loaded under the dry state in a sequence of five load steps up to the vertical stress of 74.2 kPa. Under this constant stress the specimen was wetted until a saturation of 68.99% was achieved. Wetting was completed after 35 min and specimen #3 was still left until 24 h was reached under the same vertical stress of 74.2 kPa, while recording the evolution of settlements caused by wetting. Then the load steps L6 and L7 were applied under drained condition according to the general loading program for all three specimens.

The physical parameters of the specimen before loading are summarized in Table 3 where, ρ denotes the bulk density, w the moisture content, ρ_d the dry density, ρ_s the average solid particle density, e_0 the initial void ratio, and S_r the degree of saturation.

Experimental Results of Short-Term Oedometer Compression Tests

Load and Time Dependent Evolution of Compression

For the three tested specimens #1, #2 and #3 the load and time dependent evolution of settlements are presented in Fig. 5.

It is clearly visible that the maximum immediate compression occurred in the first load step, L1, under the sitting pressure of 5.39 kPa caused by the weight of the top plate. These settlements can be attributed to the expulsion of gas and compression of very soft particles. Creep settlements

Fig. 5 Settlements versus time of the three tested specimens: specimen #1—dry; specimen #2—wet; specimen #3—dry-wet

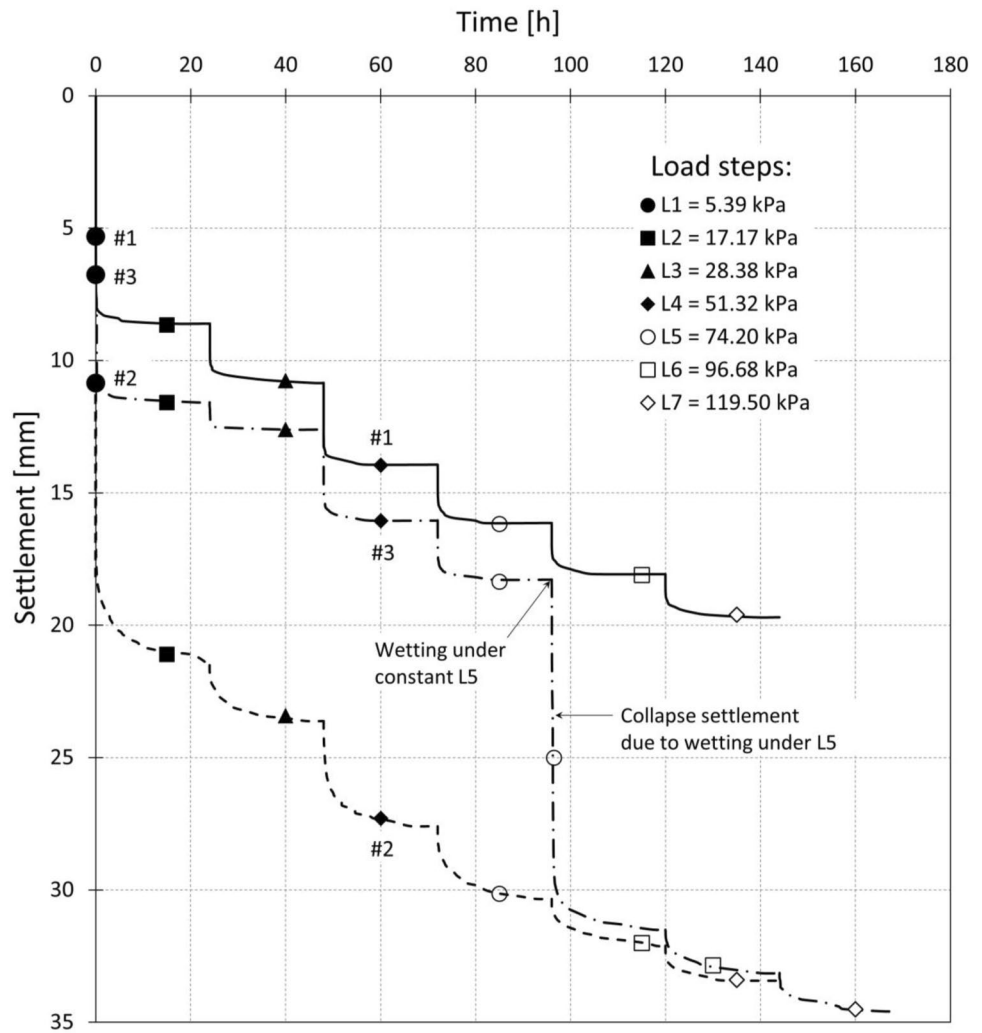


Table 4 Immediate compression of specimens #1, #2 and #3 under load step L1, i.e. under the weight of the top plate

Specimen	#1	#2	#3
Displacement [mm]	5.310	10.85	6.760
Vertical strains [%]	8.442	17.18	10.63

caused by the top plate were not investigated, because the second load increment was applied almost immediately after the placement of the top plate. For the three tested specimens the immediate compression and corresponding vertical strain caused by the top plate is shown in Table 4.

Under the load step L1 the immediate settlement is much more pronounced for the wet specimen #2 than for the dry state of specimens #1 and #3. The difference of the initial settlements of dry specimens #1 and #3 can be attributed to an inhomogeneous distribution of waste components and particle sizes within the specimen, which is an expected fact of waste material with a nature composition. This effect is

not only a question of the random distribution of each component within the mixture, but may also depend on the relation of the maximum particle sizes to the specimen size. The effect of inhomogeneous distribution of the waste mixture can presumably be reduced using larger specimens or a finer shredded waste material.

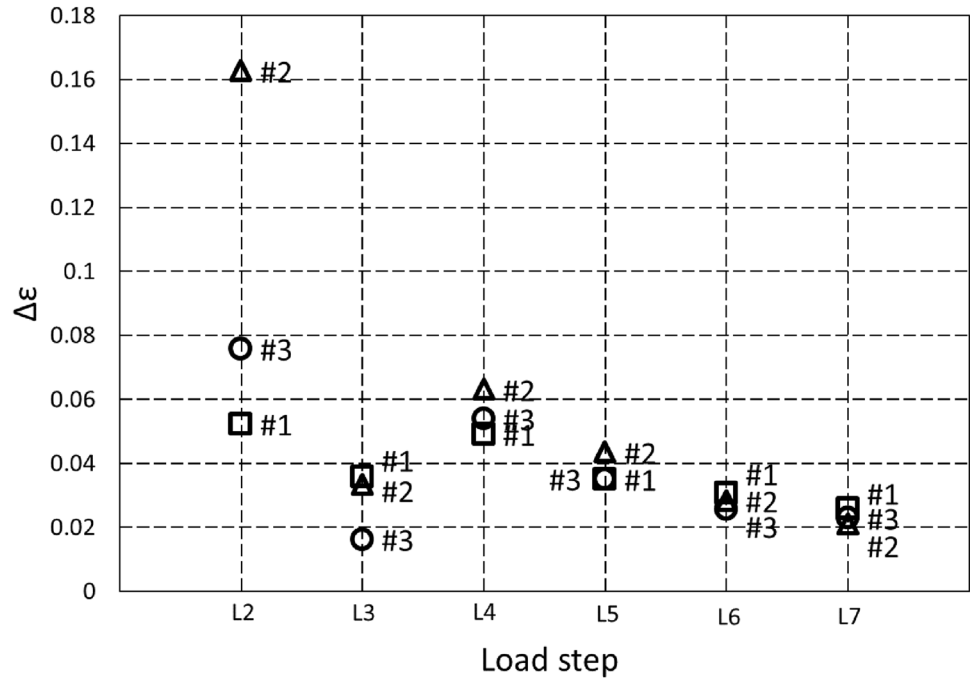
The strain increments obtained within the duration of 24 h are summarized for load steps L2 to L7 in Table 5. The strain increments include the contribution of both immediate settlement and secondary settlement. It is obvious that for all three specimens the strain increments of load step L3 are of one order less than for load step L2. For load step L4 the values are in general greater than for load step L3 which may be explained by an increase of the deformation and breakage of weak particles under this stress level. Under higher stress levels, i.e. for load steps L4 to L7, the strain increments become smaller as can be clearly seen in Fig. 6. The results also indicate the scattering of the data mainly appears within the first three load steps, i.e. up to a vertical stress of about 50 kPa. For both dry and wet specimens, the

Table 5 Strain increment within the load steps L2–L7

Specimen	L2	L3	L4	L5 dry	L5 wet	L6	L7
#1	0.0523	0.0356	0.0491	0.0350		0.0307	0.0259
#3	0.0758	0.0162	0.0539	0.0351	0.2082**	0.0256**	0.0228**
#2	0.1626	0.0334	0.0630	0.0434		0.0280	0.0209

**Specimen #3 in the wet state

Fig. 6 Strain increment ϵ_v within the load step L2–L7 of specimens #1, #2 and #3



amount of strain increments is rather close to each other in the load steps L6 and L7. Thus, it can be concluded that the strain increments under higher stresses are not significant influenced by the moisture content of previous loading conditions.

The overall strain depending on the applied vertical stress are shown in Fig. 7. In particular, the data of load steps L2–L7 are related to the states of compression the specimen was lasted 24 h under the same vertical stress. The strain increases nonlinear with increasing load. The overall compaction of the wet specimen #2 is more pronounced than the dry specimen #1. specimen #3 in its dry state showed behaviour similar to the specimen #1 while in its wet state its behaviour was similar to the specimen #2. Wetting of the specimen #3 at the preloading stress of L5 = 74.2 kPa leads to a significant compaction which is usually called collapse settlement. The mechanisms of collapse settlements are most probably due to softening of hydrophilic waste particles and particle contacts caused by wetting. In addition, a reduction of friction among the waste particles and along the wall of the oedometer cell may also cause additional rearrangement of particles into a denser formation. After increasing the saturation of the waste material from 44 to

100% a significant jump of the settlement was also reported by Basha et al. [12]. At the end of wetting a continuous loading of specimen #3 follows close to the compression curve of the initially wet specimen #2. It is also of interest to note that a similar behaviour was also observed in experiments with weathered, moisture sensitive coarse grained rockfills, e.g. [74–76]. While in the stress strain representation in Fig. 7 the wetting induced settlement appears as a jump, closer inspections show that the so-called collapse settlements are time dependent, which is clearly visible in a semi-logarithmic representation of the strain versus time scale as discussed in "Mechanical creep". In Fig. 5 this behaviour is indiscernible, because of the selected coarse resolution for the linear time scale in hours.

The oedometric compression modulus, M_{oed} , for the stress increment between two load states is defined as:

$$M_{oed} = \frac{\Delta\sigma_v}{\Delta\epsilon_v} \tag{1}$$

where $\Delta\sigma_v$ is the increment of the vertical stress and $\Delta\epsilon_v$ is the strain increment encountered 24 h after the stress increment was applied. The obtained oedometric moduli for the

Fig. 7 Vertical strain ϵ_v vs. vertical stress σ_v of specimens #1, #2 and #3

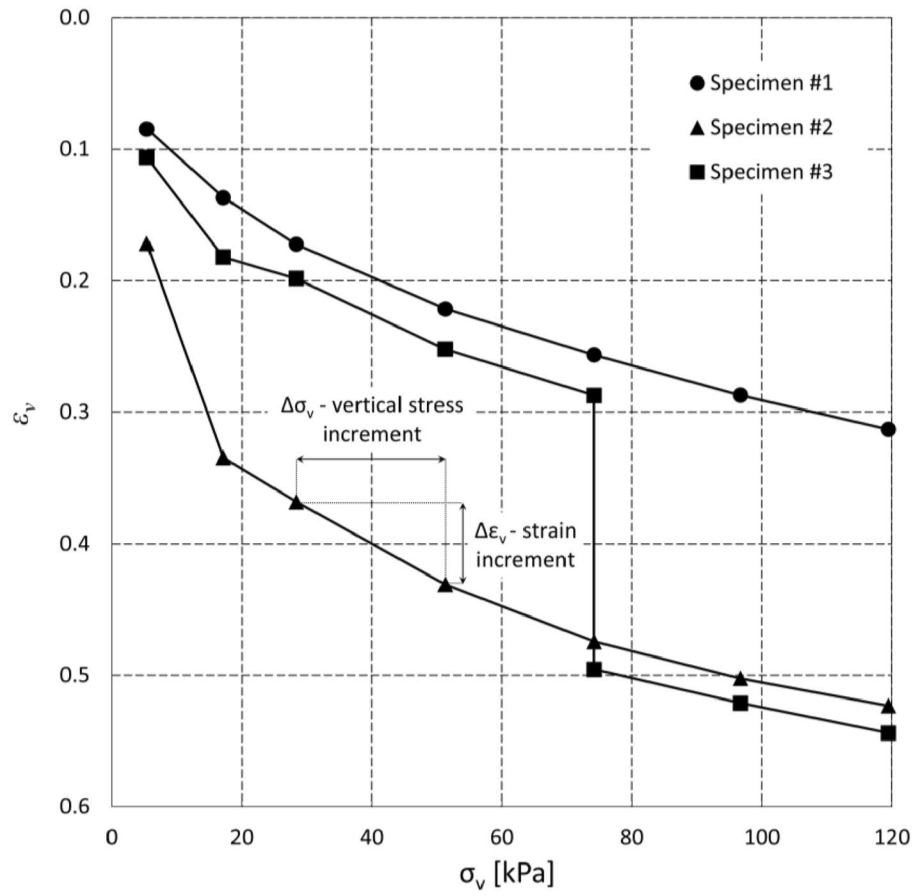


Table 6 Oedometric moduli M_{oed} of specimens #1, #2 and #3

Load step	L1	L2	L3	L4	L5	L6	L7
Stress range [kPa]	0–5.39	5.39–17.17	17.17–28.38	28.38–51.32	51.32–74.2	74.2–96.68	96.68–119.5
Oedometric modulus [kPa]							
Specimen #1	63.85	225.22	314.78	466.97	654.16	732.64	880.27
Specimen #2	31.37	72.43	335.50	363.99	527.33	802.04	1091.04
Specimen #3	50.71*	155.44*	692.19*	425.36*	652.54*	877.13**	1001.64**

*Specimen #3 in the dry state
 **Specimen #3 in the wet state.

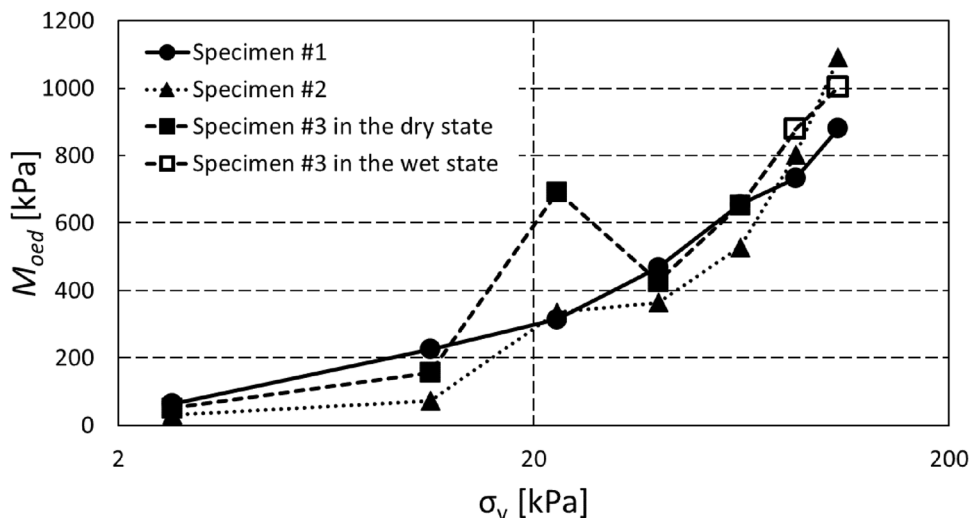
six stress states of the three specimens are summarized in Table 6. Figure 8 clearly shows the nonlinear increase of M_{oed} with an increase of the vertical stress.

Various empirical functions are proposed in the literature to approximate the strain ϵ_v as a function of the applied stress σ_v . A common approach is the representation of the strain versus the logarithmic stress by a straight line. The slope of the line is defined by the so called modified compression index C'_c :

$$C'_c = \frac{\epsilon_v}{\log(\sigma_v/\sigma_{v0})} \tag{2}$$

Herein σ_{v0} denotes the pre-existing vertical stress in the specimen prior the first load step, i.e. for $\epsilon_v = 0$. In Fig. 9 it is clearly visible, especially for the dry state of the material, that for the considered pressure range the experimental data don't fit well the linear approximation using Eq. (2). A similar behaviour was also observed in experiments by Zhang

Fig. 8 Stress dependent oedometric moduli, M_{oed} , of specimens #1, #2 and #3. (The location of the shapes is related to the vertical stress σ_v in the middle of the corresponding stress interval $\Delta\sigma_v$)



et al. [36] with a MBT waste material from China. In an attempt to get closer approximation to experimental data the pressure dependent oedometer modulus equation proposed by Ohde [77] and Janbu [78] is proposed, i.e.

$$E^{oed} = E_r^{oed} \left(\frac{\sigma_v}{\sigma_{vr}} \right)^\beta \tag{3}$$

where the reference modulus E_r^{oed} is related to the corresponding vertical stress $\sigma_v = \sigma_{vr}$. With respect to $d\sigma_v = E^{oed} d\varepsilon_v$ the integration of this differential equation leads (Bauer [79]):

$$\varepsilon_v = \varepsilon_r \left(\frac{\sigma_v}{\sigma_{vr}} \right)^{(1-\beta)} \tag{4}$$

Herein ε_r denotes the reference strain at the reference stress σ_{vr} , i.e. $\varepsilon_r = \sigma_{vr} / (E_r^{oed} (1 - \beta))$. The experimental data together with the approximation function (4) is shown in Fig. 10. The approximation functions (2) and (4) are compared in a semi-logarithmic representation in Fig. 9.

Based on the strain–stress relationship approximated by Ohde’s function also a smooth representation of the stress dependent oedometer modulus $E^{oed}(\sigma_v)$ can be obtained. With respect to Eq. (4) Ohde’s Eq. (3) can be rewritten to:

$$E^{oed} = \frac{\sigma_{vr}}{\varepsilon_r (1 - \beta)} \left(\frac{\sigma_v}{\sigma_{vr}} \right)^\beta \tag{5}$$

In particular, the following approximation functions are obtained: for the dry specimen #1:

$$E^{oed} = \frac{119.5}{0.313046(1 - 0.58)} \left(\frac{\sigma_v}{119.5} \right)^{0.58} \tag{6}$$

and for wet specimen #2:

$$E^{oed} = \frac{119.5}{0.523212(1 - 0.724)} \left(\frac{\sigma_v}{119.5} \right)^{0.724} \tag{7}$$

The corresponding relations for specimen #1 and specimen #2 are shown in Fig. 11 together with the oedometric moduli obtained by Jessberger and Kockel [2], Chen et al. [19] and Zhang et al. [36]. In particular, the data by Jessberger and Kockel [2] were obtained with fresh and decomposed raw MSW material. It should be noted that the results presented by Jessberger and Kockel [2] are derived from the virgin compression line by considering only mechanical compression. According to their results decomposed raw MSW material under the same stress level exhibits a much stiffer behaviour than the fresh raw MSW. Clearly, decomposition of organic content within the raw waste matrix leads to the loss of the light-weight and highly compressible organic particles. Consequently, void spaces emptied by the decomposition process allow inert waste particles to rearrange their position into a denser state which leads to a stiffer behaviour. The lower compressibility of decomposed waste compared to the fresh and less decomposed waste specimens are also reported by Reddy et al. [80]. Figure 11 also shows the results obtained by Reddy et al. [80] for two waste specimens with different degree of decomposition (DOD). Compared to the less decomposed specimen the more decomposed sample shows a much higher stiffness and for DOD of 86% it is higher than the upper boundary proposed by Jesberger and Kockl [2]. The oedometric moduli of raw waste obtained by Chen et al. [19] are close to the oedometric moduli for the fresh raw MSW material published by Jesberger and Kockel [2]. Zhang et al. [36] tested two MBT waste specimens from different seasons. Specimen M1 was obtained in the winter period and shows a higher stiffness in the lower stress range than that of specimen M2 which was obtained in the

Fig. 9 Compression behaviour in a semi-logarithmic representation of: (a) specimen #1; (b) specimen #2; (c) specimen #3

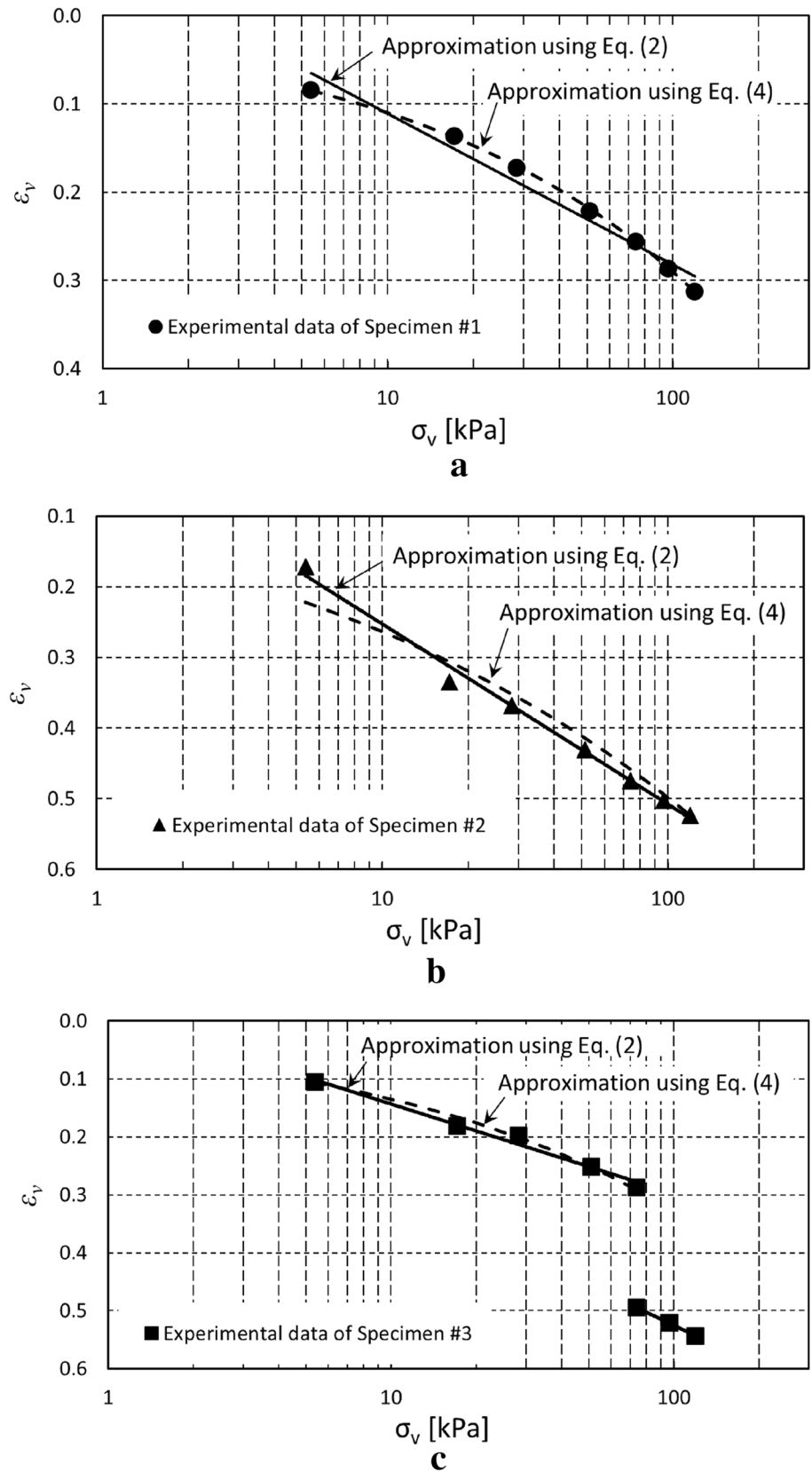


Fig. 10 Vertical strain vs. vertical stress of specimens #1 and #2: shapes denote experimental data, solid curve and dashed curve the approximation with Eq. (4)

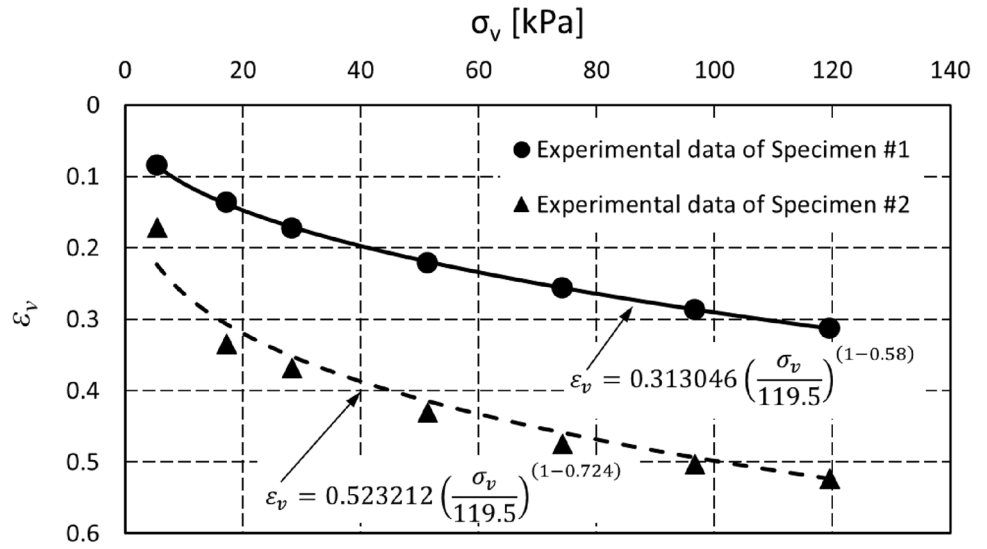


Fig. 11 Oedometric modulus depending on the vertical stress of specimen #1 and specimen #2 together with experimental data by Jessberger and Kockel [2], Chen et al. [19], Zhang et al. [36] and Reddy et al. [80]

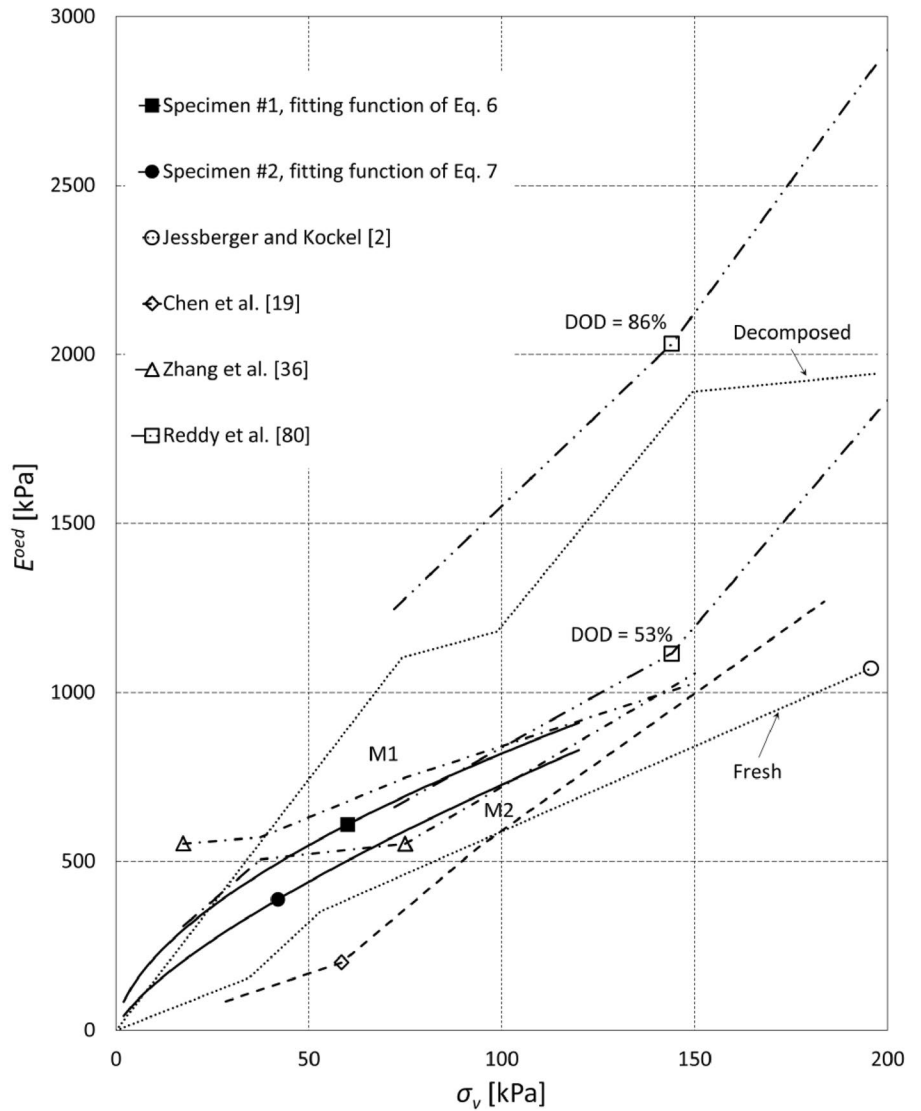


Table 7 Physical parameters of tested specimens at the end of the oedometer compression test

Specimen condition	ρ [g/cm ³]	W [%]	ρ_d [g/cm ³]	e_l	S_r [%]	ϵ_1
#1 (dry)	0.553	0	0.553	2.424	0	0.3131
#2 (wet)	1.180	56.61	0.754	1.376	77.92	0.5232
#3 (dry–wet)	1.237	56.93	0.788	1.274	84.64	0.5438

summer period. The results in Fig. 11 show that the stiffness moduli of the dry and wet MBT waste material of the present research, i.e. specimen #1 and specimen #2, lie within the range of the of published values by Jessberger and Kockel [2] for the fresh and decomposed raw MSW material.

Physical quantities at the end of the tests are presented in Table 7. Under the maximum vertical load the dry specimen #1 gained a vertical strain of 31.3% while for the initially wet specimen #2 the obtained vertical strain was 52.3%. Consequently, the final void ratios e_l of wet specimens #2 and #3 are much lower than for the dry specimen #1 while the bulk density, ρ_d , of the wet specimens is significantly higher. The differences between specimens #2 and #3 maybe caused by the higher degree of saturation of specimen #3.

Distinction Between Immediate and Secondary Compression

A closer inspection of the settlement-time curves indicates that for the MBT waste material used no clear transition from the instantaneously compression to the secondary compression can be detected for both the dry and the wet states of the material. For instance, Fig. 5 shows that the settlements are time dependent immediately after a new load increment is applied. Thus, the use of terms such as “immediate compression” or “immediate settlement” for inherently time dependent processes can be misleading. As delayed settlements can also be observed for the dry state of the material the time dependent behaviour under constant load cannot be explained by mechanisms considered in classical consolidation theory. From the phenomenological perspective, it can therefore be suspected that certain components of the MBT waste mixture exhibit an inherently viscous behaviour. As no clear distinction between immediate and secondary compression can be gathered from the course of the settlement-time curves within each load step several pragmatic rules are proposed in the literature to define a fictitious time, EOT, at which the compression behaviour transitions from immediate compression to secondary compression (e.g. [63–66]). As biodegradation is avoided during the whole test, the secondary compression is only caused by mechanical creep. Although EOT is not a physical quantity, a distinction between immediate and secondary compression can for instance be of practical interest for the formulation of simple bi-linear compression models. For the tested specimens in

the present research the following four different methods for computing the EOT values were investigated:

In the “10 s” method a fixed EOT value of 10 s is assumed after applying a new load increment. The corresponding strain is taken as ϵ_{EOT} .

According to Bareither et al. [7] in the “FORE method” the assumption is made that the mechanical creep can be represented in a semi-logarithmic representation by a straight line. In particular, the experimental data overlapped by the FORE equation and the part of data represented by a straight line in a semi-logarithmic representation are assumed to encompass the entire mechanical creep. Thus, EOT is defined for the time, the two equations become coincide. For instance, for the experimental data of the load step L4 of the wet specimen #2 the relevant FORE equation reads:

$$\epsilon_v = 10^{(-0.0011t-1.5678)} + 0.0636 \quad (8)$$

and the semi-logarithmic equation, SLE, for the part of experimental data approximated by a straight line reads: $\epsilon_v = 0.0089 \ln(t) + 0.0007$ (9)

In Eqs. (8–9) the time is given in minutes. The results of the two equations together with the experimental data are shown in Fig. 12. On following the proposed procedure the values obtained are EOT = 110 min and $\epsilon_{EOT} = 0.0428$.

In order to overcome the influence of the scattering of experimental data on the estimated EOT value, the method outlined in (b) is applied to the smoothed representation of the experimental data. In particular, for the stress level L4 of specimen #2 the strain vs. time data are approximated by the following equation, SAE: $\epsilon_v = 0.0072 \ln(t) + 0.0113$ (10)

The corresponding FORE equation reads:

$$\epsilon_v = 10^{(-0.0007t-1.6308)} + 0.066 \quad (11)$$

Based on the smoothed curves shown in Fig. 13 a value of EOT = 140 min and a value of $\epsilon_{EOT} = 0.0475$ are obtained. Compared to the results in Fig. 12 obtained with the raw data, even though the EOT time is higher the differences in the obtained values were negligible.

In the “strain-rate method” (SRM) the determination of the EOT values are based on a specific strain rate, which is assumed to be the same for all load steps. The proposed method is motivated by the observation that under the same initial moisture content the strain rate of mechanical creep is not significantly affected by the stress level. With the assumption that mechanical creep can be approximated by

Fig. 12 Vertical strain ϵ_v vs. time t for the stress level L4 of specimen #2: shapes denote experimental data, dash-dotted curve dashed-dotted curve is related to the FORE method, and the dashed line denotes the SLE approximation

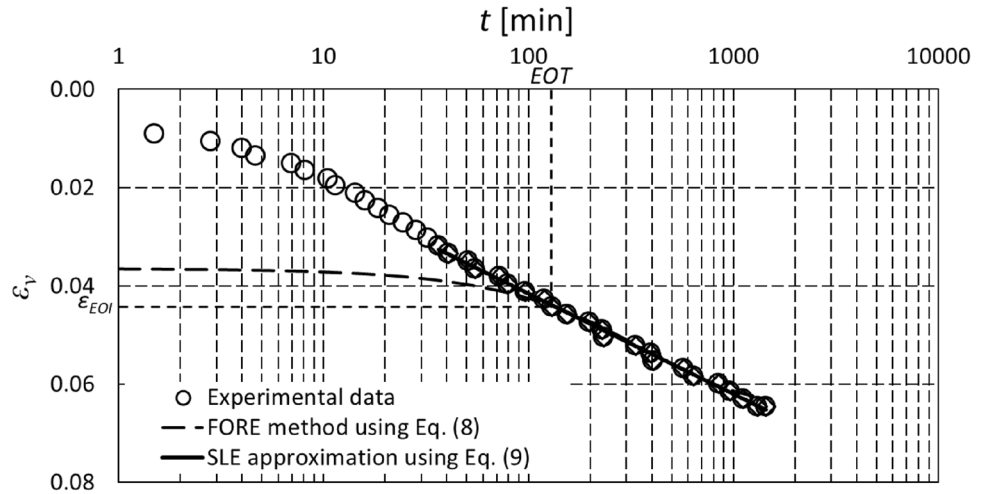
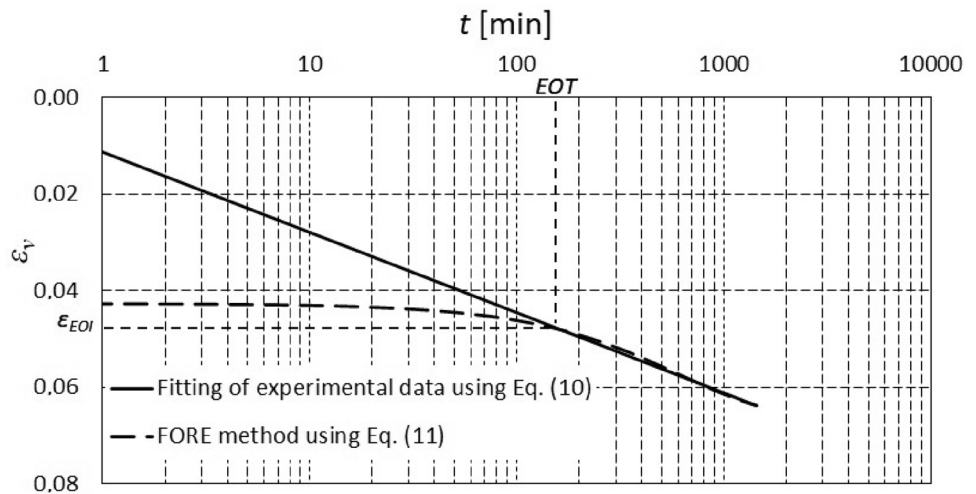


Fig. 13 Vertical strain ϵ_v vs. time t for the stress level L4 of specimen #2: the solid curve denotes the fitting of the experimental data, and the dash-dotted curve is related to the FORE method

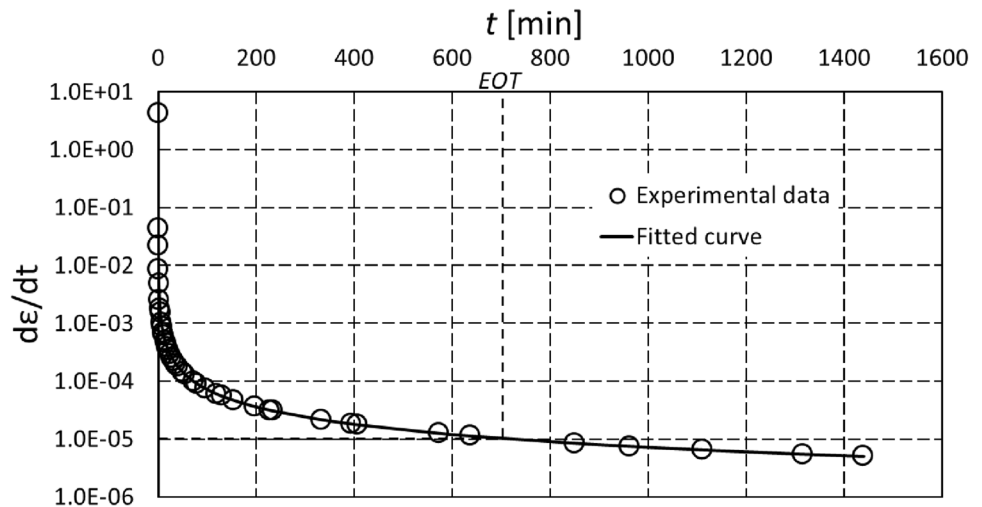


a single creep ratio the EOT values obtained with SRM are similar to those of the methods described in (b) and (c). However, compared to the methods described in (b) and (c) the procedure required for SRM is simpler. In this paper the SRM is applied to smoothed strain vs. time. The strain rate vs. time curve can be obtained either analytically or from the numerical time derivative of the strain vs. time curve. The reference strain rate was assumed for the state and the reduction of the strain rate with time turns almost into a straight line, i.e. the state in which the retardation of the strain rate takes on an almost constant value. As the strain rate did not significantly vary for the other load steps a fixed value of 0.00001 min^{-1} was assumed for all load steps and for both the dry and the wet states of the material. Figure 14 shows the procedure for estimating EOT for the data of the load step L4 of the wet specimen #2. In particular, for a strain rate of 0.00001 min^{-1} the value of $EOT = 700 \text{ min}$.

The EOT values obtained for the different methods are summarized in Table 8 for the three tested specimens and

the load steps L2 to L7. The comparison of the different methods shows, that the value of EOT is different for the dry and the wet material and it also depends on the applied load. Thus, a method with a fixed value of EOT, such as is assumed in the “10 s” method, cannot be recommended for the calculation of the strain, ϵ_{EOI} , the material turns from immediate to secondary compression. Using the FORE method the differences between ϵ_{EOI} strains obtained from method (b) and method (c) in most cases are less than 10% even though the corresponding EOI values differ significantly. Interestingly, the ϵ_{EOI} values obtained with the SRM method on dry samples do not significantly differ from the ϵ_{EOI} values obtained with the FORE method. For the wet specimen #2, however, the SRM method provided higher EOT and ϵ_{EOI} values than for the FORE method. The transition from immediate to secondary compression occurs at higher values of EOT for the wet than for the dry specimen. It can be noted that in all methods the end-of-time for the dry state of the specimens scatters significantly for lower load

Fig. 14 Time derivative of the strain vs. time for the stress level L4 of specimen #2



steps up to 50 kPa. This fluctuation can most probably be attributed to the effect of a locally higher contact resistance between the heterogeneous distribution of particular waste components. At higher load steps the corresponding values of ε_{EOI} does not deviate strongly for the considered methods (b)-(d). The consequences of the different EOT methods on the calculated modified secondary compression indexes are discussed in the next subsection.

Mechanical Creep

The time dependent evolution of the vertical strain for the load steps L2 to L7 is shown in the semi-logarithmic representation for specimens #1, #2 and #3 in Figs. 15, 16 and 17, respectively. In that the vertical strains represents the total values and the time scale denotes the time interval of 24 h within the load steps are kept constant. The onset of the mechanical creep phase depending on the EOT method discussed in "Distinction Between Immediate and Secondary Compression" is indicated for each individual load step by corresponding markers. Shortly after applying the additional load the inclination of the creep curves reaches almost from the same order as that of the dry specimen #1. Compared to the dry specimen the inclination of the creep curves of the wet specimen #2 are greater, which reflects the combined process of both consolidation and creep and it is more pronounced for the load step L2 than for the other subsequent load steps. Specimen #3 shows in the dry state a sudden significant change of the strain velocity at about 8 min after applying load step L2 which may be related to a delayed reaction of an inhomogeneous arrangement of viscous particles within the particle skeleton of the specimen. Compared to specimen #1 the total strain increment of specimen #3 under load step L2 is significantly greater, which is an indicator of the difficulties to be faced in reproducing experimental data under low stress levels. Under the higher

stress levels of load steps L3, L4 and L5 the corresponding stress increments obtained with specimen #1 and specimen #3 are more similar. Wetting of the initial dry specimen #3 was carried out under the constant pre-compressed vertical stress of 74.2 kPa within 35 min as outlined in more details in "Testing Procedure". The wetting phase shows a rather uneven change of the strain velocity, which may be caused by slow wetting of the specimen from the bottom to the top. The course also indicates that wetting induced settlements, frequently referred to as "collapse settlements", are time dependent. Sequence loadings under L6 and L7 lead within the investigated time interval to strain increments similar to both specimen #3 and specimen #2.

For a detailed quantification of the mechanical creep it is assumed that the corresponding time dependent settlements under constant vertical stress can be represented by the so-called modified secondary compression index, $C'_{\alpha,\varepsilon}$, which is defined as:

$$C'_{\alpha,\varepsilon} = \frac{\Delta\varepsilon}{\log(t/t_1)} \quad (12)$$

In Eq. (12) $\Delta\varepsilon$ denotes the creep stain induced within the time interval $t-t_1$ of the secondary compression phase and t_1 is the time for completion of the immediate settlements. With respect to the EOT methods (a), (b) and (c) outlined in "Distinction between immediate and secondary compression" the value of $C'_{\alpha,\varepsilon}$ calculated for the load steps L2–L7 are summarized in Table 9. The results for the specimen #1 and Specimen #2 are also visualized in Fig. 18a, b, respectively. It is clearly visible that for the dry specimen the "10 s method" provides higher values for $C'_{\alpha,\varepsilon}$ than the "FORE method" and the "strain rate method", while for the wet specimen the behaviour is largely revised. As for the wet specimen #2 the course under load step L3 seems to be rather unrealistic and it is

Table 8 End-of-immediate compression time, EOT, and corresponding strain, ϵ_{EOT} , for applied methods (a-d), and the load steps (L2-L7) of specimens #1, #2, and #3

Load step	L2		L3		L4		L5		L6		L7	
	EOT [min]	ϵ_{EOT} [-]	EOT [min]	ϵ_{EOT} [-]	EOT [min]	ϵ_{EOT} [-]	EOT [min]	ϵ_{EOT} [-]	EOT [min]	ϵ_{EOT} [-]	EOT [min]	ϵ_{EOT} [-]
Specimen #1	(a)	0.167	0.0330	0.0123	0.167	0.0262	0.167	0.0137	0.167	0.0108	0.167	0.0061
	(b)	60	0.0464	0.0294	80	0.0440	100	0.0300	48	0.0237	240	0.0219
	(c)	60	0.0445	0.0323	87	0.0423	75	0.0287	125	0.0261	200	0.0216
	(d)	300	0.0494	0.0319	325	0.0473	250	0.0316	225	0.0275	190	0.0215
Specimen #2	(a)	0.167	0.074	0.0030	0.167	0.0046	0.167	0.0050	0.167	0.0030	0.167	0.0032
	(b)	80	0.1268	0.0273	110	0.0428	200	0.0284	160	0.0156	180	0.0147
	(c)	120	0.1328	0.0231	140	0.0475	130	0.0267	145	0.0160	95	0.0122
	(d)	900	0.1529	0.0279	700	0.0550	700	0.0388	500	0.0221	450	0.0186
Specimen #3	(a)	0.167	0.0096	0.0024	0.167	0.0280	0.167	0.0010	0.167	0.0010	0.167	0.0030
	(b)	100	0.0698	0.0153	60	0.0476	80	0.0300	60	0.0113	270	0.0159
	(c)	110	0.0662	0.0138	80	0.0476	60	0.0294	160	0.0193	220	0.0166
	(d)	450	0.0725	0.0145	350	0.0512	225	0.0319	260	0.0205	350	0.0160

neglected in Figs. 18b and 19. In summary it can be concluded that compared with the “10 s method” the “FORE method” and “strain rate method” yield, for the wet specimen, higher values for $C_{\alpha,\epsilon}$ under the same stress state. It is obvious that the values of $C'_{\alpha,\epsilon}$ obtained from the different EOT methods show greater differences for the load increments L2-L4, but it become lesser for higher stresses, i.e. under higher stresses the investigated EOT methods lead to $C'_{\alpha,\epsilon}$ values which are relatively close to each other.

In order to visualize the trend of the evolution of the pressure dependent modified secondary compression index, the mean values of $C'_{\alpha,\epsilon}$ obtained from the investigated EOT methods (a)–(d) were fitted by a linear approximation. The corresponding functions for the dry specimen #1 and the wet specimen #2 read $C_{\alpha,\epsilon}^{l,mean} = -1.058 \times 10^{-6} \sigma_v + 0.0049$ and $C_{\alpha,\epsilon}^{l,mean} = -0.0001213 \times 10^{-4} \sigma_v + 0.0235$, respectively. From the linear fitting shown by a solid line in Fig. 18 it can clearly be seen that the average value of $C'_{\alpha,\epsilon}$ is higher for the wet specimen #2 and it decreases with increasing stress. On the other hand for the dry specimen #1 the decrease of $C'_{\alpha,\epsilon}$ with increasing stress is very small and influenced by the data scattering of data for lower stresses.

A comparison of the stress dependent mean values of the modified secondary compression index obtained in the present study with data published in the literature is shown in Fig. 19. In particular, the data by Hyun et al. [30] were obtained from an untreated 10 years old municipal solid waste with a maximum particle size of 4.8 mm and a mean particle size of about 2.5 mm. The tested specimen was in a wet state. Siddiqui et al. [62] investigated two different MBT waste materials, i.e. a specimen from an MBT plant located in Southern England (UK) and a specimen from an MBT plant located in Northern Germany (GER). The former of the two was an aerobically degraded MBT waste with maximum particle size of about 20 mm. The maximum particles size of the later was 60 mm. The granulometric curves of waste samples used by Siddiqui et al. [62] can be found by Velkusanova [29] which are also presented on Fig. 3. During testing the samples were fully submerged and subjected to a leachate recirculation process. Jessberger and Kockel [2] tested 15 years old untreated municipal solid waste material in an unsaturated state. Although different waste materials are used in the experiments shown in Fig. 19 the results are within the stress range obtained in the present investigations. It can also be noted that for the present experimental investigations the value of $C'_{\alpha,\epsilon}$ decreases for the moist waste material but it is almost constant for the dry material. A similar tendency for the wet specimen #2 can also be observed from the experimental data by Siddiqui et al. [62] obtained from wet specimens in Southern England (UK) and

Fig. 15 Creep curves under the individual load steps L2–L7 of specimen #1

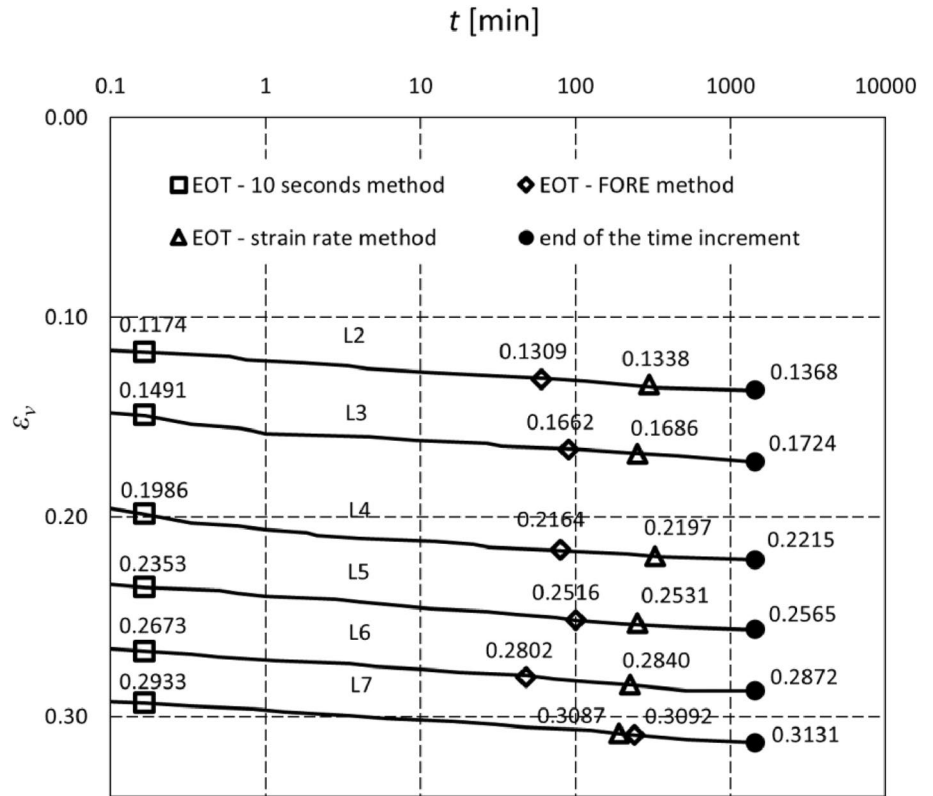


Fig. 16 Creep curves under the individual load steps L2–L7 of specimen #2

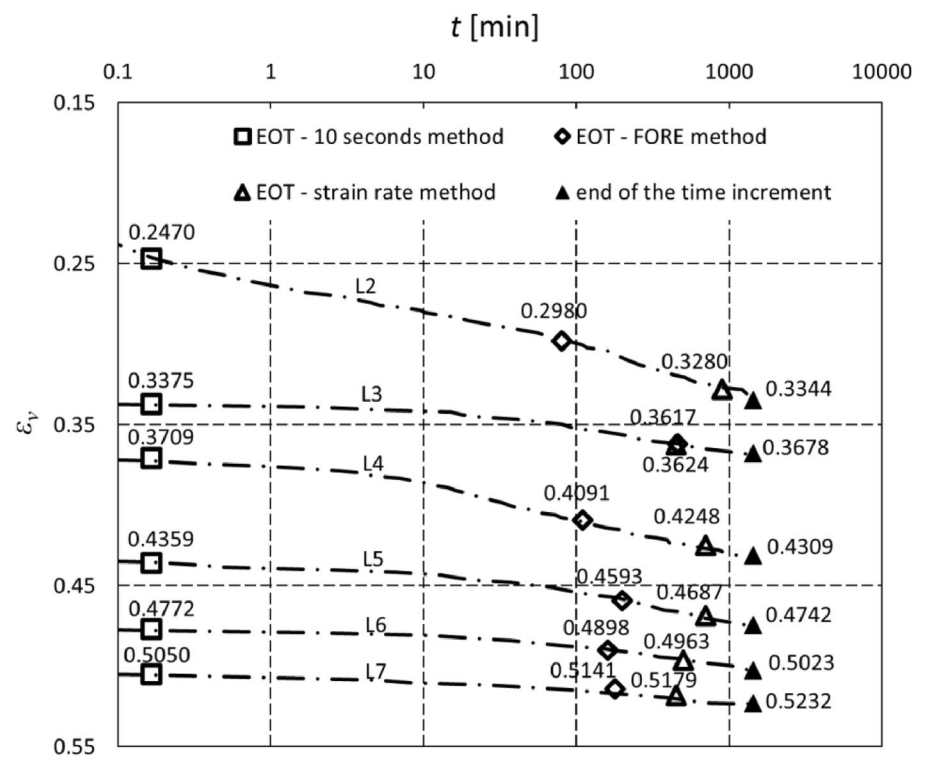


Fig. 17 Creep curves under the individual load steps L2–L7 of specimen #3

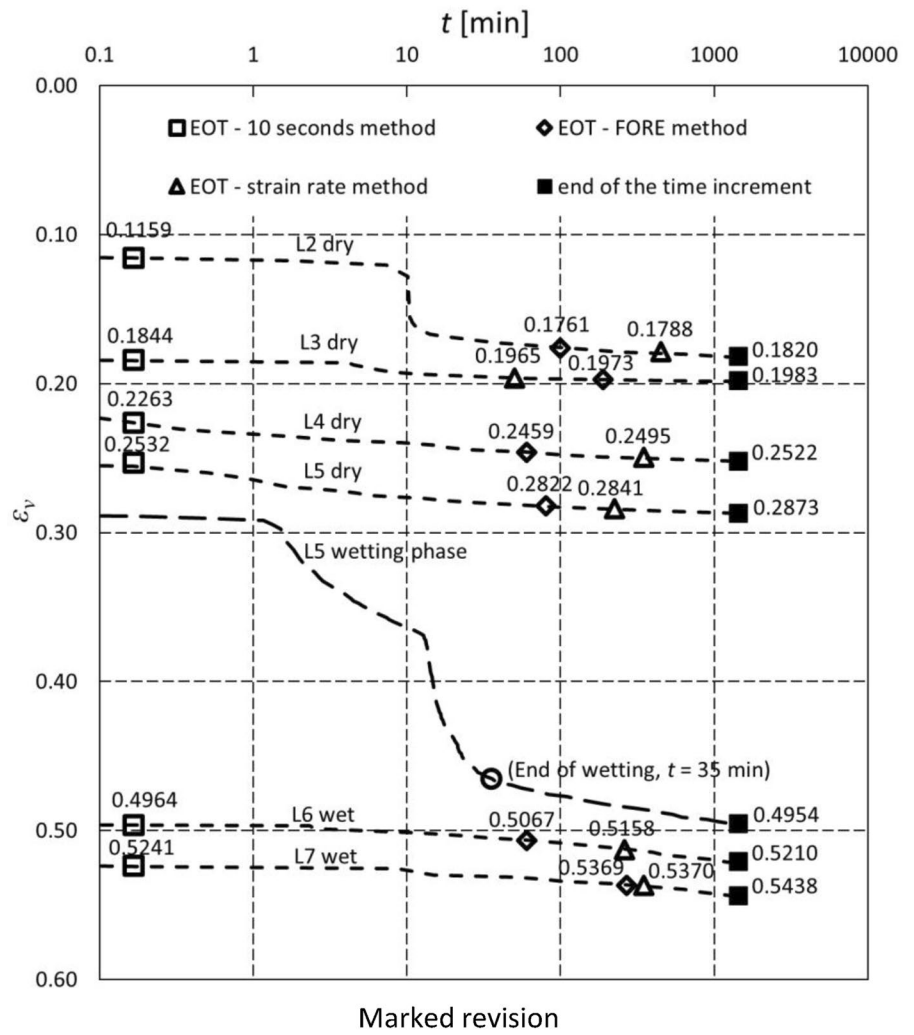


Table 9 Modified secondary compression indexes $C'_{\alpha,\epsilon}$ for individual load steps L2–L7 and for the EOT methods (a), (b), (c) and (d)

Load step	L2	L3	L4	L5	L6	L7	
Specimen #1	(a)	0.0049	0.0059	0.0058	0.0054	0.0051	0.0050
	(b)	0.0042	0.0052	0.0041	0.0043	0.0047	0.0051
	(c)	0.0057	0.0049	0.0056	0.0049	0.0043	0.0050
	(d)	0.0043	0.0050	0.0028	0.0045	0.0040	0.0050
Specimen #2	(a)	0.0208	0.0077	0.0152	0.0096	0.0064	0.0052
	(b)	0.0236	0.0123	0.0195	0.0174	0.0130	0.0100
	(c)	0.0219	0.0103	0.0168	0.0160	0.0121	0.0098
	(d)	0.0171	0.0107	0.0194	0.0176	0.0130	0.0104
Specimen #3	(a)	0.0168	0.0035	0.0066	0.0087	0.0063	0.0050
	(b)	0.0052	0.0011	0.0046	0.0040	0.0104	0.0095
	(c)	0.0086	0.0013	0.0050	0.0041	0.0067	0.0076
	(d)	0.0065	0.0012	0.0044	0.0039	0.0070	0.0110

Northern Germany (GER). However, the way in which the moisture content, the particle size distribution, the history

of pre-treatment, and aging influence the stress dependency of $C'_{\alpha,\epsilon}$ is still an open question.

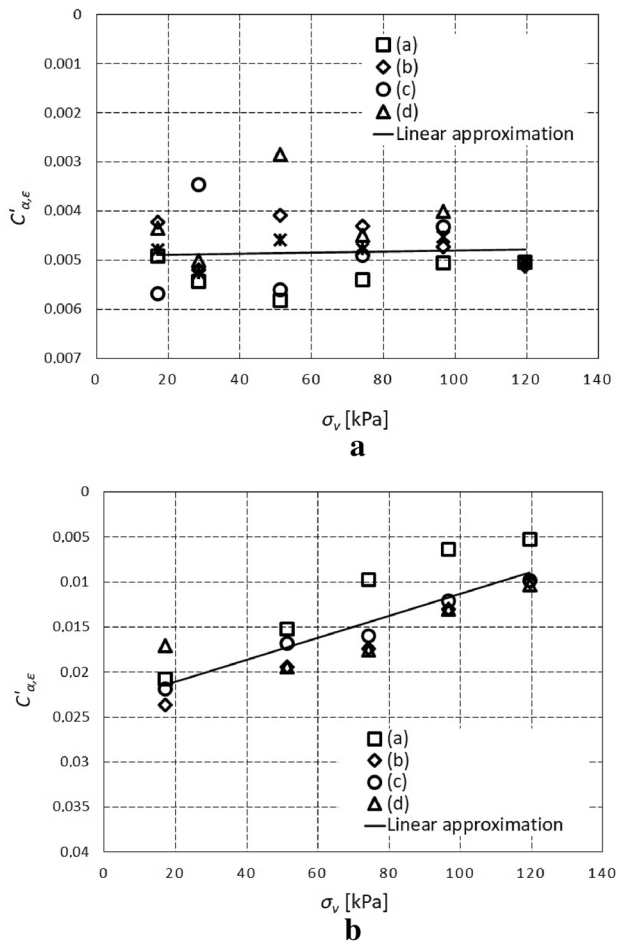


Fig. 18 Modified secondary compression index, $C'_{\alpha, \epsilon}$, vs. vertical stress, σ_v , for the investigated methods (a-d) and for particular load steps of: (a) specimen #1; (b) specimen #2

Conclusions

In this paper the time dependent compression behaviour of an initially dry and of an initially wet state of a mechanically treated and biologically dried waste material with a methanogenic fraction was investigated in an adapted oedometer device with a specimen diameter of 150 mm. The waste material had a mean particle diameter of approximately 6 mm and was composed mainly of plastic, paper, textiles, glass, metal, wood, stones, ceramics and kitchen waste. In order to investigate only the purely mechanical response, in the experiments biodegradation of the wet specimen was suppressed with an addition of acetic and propionic acids to the waste material. The maximum vertical stress of 119.5 kPa was applied in a sequence of seven load steps, with each load step being kept constant for 24 h. The maximum vertical stress was applied to each specimen during a total duration of 7 days and in the context of the applied specimen preparation for preventing biodegradation

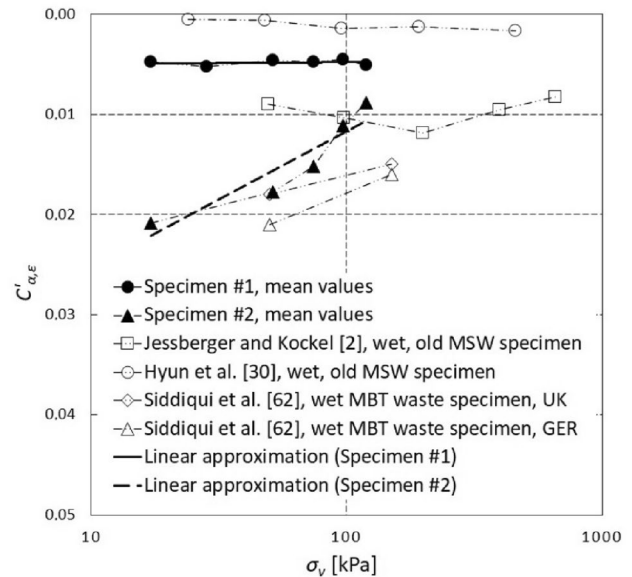


Fig. 19 Mean value of the modified secondary compression index, $C'_{\alpha, \epsilon}$, vs. vertical stress, σ_v , and for particular load steps of specimen #1 and specimen #2 compared with data published

processes a notable change of the specimen temperature can be excluded. Thus, the experimental results can be assigned as short-term compression tests under constant temperature.

For the interpretation of the experimental data a distinction is made between the oedometric compression modulus, the modified compression index and the modified secondary compression index. It is shown that a reformulation of the compression law by Ohde, originally proposed for sand, permits a closer approximation of the experimental data than the modified compression index. With help of Ohde's law a smooth representation of the stress dependent oedometer modulus could be obtained for the testes stress range.

The paper also considers a more detailed discussion of the distinction between immediate and secondary compression. The settlements are time dependent already at the onset of each new load increment for both the dry and the wet material. The waste material used thus exhibits an inherently viscous behaviour and a distinction between immediate and secondary compression using a fictitious time, which is more pragmatic than physical. Various concepts for choosing a fictitious time were investigated with regards to their influence on the modified secondary compression index. Apart from some common methods such as the "FORE method" a new method with the name "Strain-rate method" was proposed, which assumes a fictitious strain rate where immediate compression turns into mechanical creep. While in the "FORE method" the fictitious time is estimated based on strain vs. time scale in a semi-logarithmic representation, in the "Strain-rate method" the strain rate is chosen based on the strain-rate-time scale in a linear representation.

For the latter values that were a little higher were obtained for the fictitious time and also for the modified secondary compression index. Furthermore, it can also be noted that for the tested material the value of the modified secondary compression index decreases for the wet material but it is almost constant for the dry material. Although the results of the stress dependent oedometric modulus and the modified secondary compression index lay within the range of experimental data published by other authors, the way in which the portion of individual waste components of the mixture, moisture content, particle size distribution and history of pre-treatment influences the mechanical parameter it is still an open question.

In addition, the so-called collapsibility behaviour caused by wetting of the initially pre-compressed material under dry condition was also investigated. A closer inspection of the time scale shows that wetting deformation is also time dependent. It is of interest to note that after wetting a continuous loading follows close on the compression curve of the initially wet specimen. A similar behaviour was also observed in experiments with weathered, moisture sensitive coarse grained rockfills.

Authors Contributions Nikola Kaniski and Nikola Hrcic conducted the oedometer test on Marišćina MBT waste and analysed the compression behaviour transitions from immediate to secondary compression. Erich Bauer and Igor Petrovic analysed the test data and reviewed and revised the full manuscript. All authors read and approved the final manuscript.

Funding The financial support of the Croatian Ministry of Science and the Austrian Federal Ministry of Science, Research and Economy and the support of the OeAD Scientific and Technological Cooperation (WTZ Project: HR 01/2018 “Numerical modelling of the long-term behaviour of biostabilised MBT waste material”) financed by the Austrian Federal Ministry of Science, Research and Economy (BMFWF) is gratefully acknowledged. Further support of the Croatian Science Foundation for the project “Testing and modelling of mechanical behaviour of biodried waste as a Waste-to-Energy prerequisite” (UIP-2017-05-5157) is also gratefully acknowledged.

Data Availability The datasets generated during and/or analysed during the current study are available in the Dabar repository, <https://urn.nsk.hr/urn:nbn:hr:130:817727>”.

Declarations

Competing interests The authors have no relevant financial or non-financial interests to disclose.

References

1. Waste Framework Directive: <https://ec.europa.eu/environment/waste/framework/> (accessed 30 July 2022)
2. Jessberger, H. L. and Kockel, R.: Determination and Assessment of the Mechanical Properties of Waste Materials. In: Proceedings of Sardinia 93, 4th International Landfill Symposium, S. Margherita di Pula, Cagliari (1993)
3. Hossain, S.: Mechanics of Compressibility and Strength of Solid Waste in Bioreactor Landfills, PhD thesis, Faculty of North Carolina State University at Raleigh (2002)
4. Sivakumar Babu, G.L., Reddy, K.R., Chouksey, S.K.: Constitutive model for municipal solid waste incorporating mechanical creep and biodegradation-induced compression. *Waste Manage.* **30**, 11–22 (2010)
5. Stoltz, G., Gourc, J.-P., Oxarango, L.: Characterisation of the physico-mechanical parameters of MSW. *Waste Manage.* **30**, 1439–1449 (2010). <https://doi.org/10.1016/j.wasman.2010.03.016>
6. Drut N., Gourc, J. P., Staub, M., Stoltz, G., Mansour, A.: Large-scale oedometers (ciclades) for monitoring the long-term hydro-mechanical behaviour of MSW, Fourth International Workshop “Hydro-Physico-Mechanics of Landfills” Santander, Spain; 27–28 April (2011)
7. Bareither, C.A., Benson, C.H., Edil, T.B.: Compression behavior of municipal solid waste: immediate compression. *J. Geotech. Geoenviron. Eng.* **2012**(138), 1047–1062 (2012)
8. Bareither, C.A., Benson, C.H., Edil, T.B., Barlaz, M.A.: Abiotic and biotic compression of municipal solid waste. *J. Geotech. Geoenviron. Eng.* **2012**(138), 877–888 (2012)
9. Bareither, C.A., Breitmeyer, R.J., Benson, C.H., Barlaz, M.A., Edil, T.B.: Deer track bioreactor experiment; field-scale evaluation of municipal solid waste bioreactor performance. *J. Geotech. Geoenviron. Eng.* **2012**(138), 658–670 (2012)
10. Bareither, C.A., Benson, C.H., Edil, T.B.: Compression of municipal solid waste in bioreactor landfills: mechanical creep and biocompression. *J. Geotech. Geoenviron. Eng.* **2013**(139), 1007–1021 (2012)
11. Karimpour-Fard, M., Lemos, M.S.: Deformation characteristics of MSW materials. *EJGE* **17**, 2009–2024 (2012)
12. Basha, B.M., Parakalla, N., Reddy, K.R.: Experimental and statistical evaluation of compressibility of fresh and landfilled municipal solid waste under elevated moisture contents. *Int. J. Geotech. Eng.* (2015). <https://doi.org/10.1179/1939787915Y.0000000018>
13. Hong-jun, S., Bin, C., Li-hong, Z.: Experimental study of primary compression settlement of bioreactor landfills. *Open Civ. Eng. J.* **9**, 1012–1015 (2015)
14. Reddy, K.R., Hettiarachchi, H., Giri, R.K., Gangathulasi, J.: Effects of degradation on geotechnical properties of municipal solid waste from Orchard Hills Landfill, USA. *Int. J. Geosynth. Ground Eng.* **1**(24), 15 (2015). <https://doi.org/10.1007/s40891-015-0026-2>
15. Zhang, Z., Wu, D., Yan, L., Ding, Z., Wang, Y., Lei, S.: Experimental study on the compression properties of degraded municipal solid waste, Proceedings of the 8th International Conference on Waste Management and The Environment (2016). <https://doi.org/10.2495/WM160241>
16. Zekkos, D., Fei, X., Grizi, A., Athanasopoulos, G.A.: Response of municipal solid waste to mechanical compression. *J. Geotech. Geoenviron. Eng.* **143**(4), 1608 (2016). [https://doi.org/10.1061/\(ASCE\)GT.1943-5606.0001608](https://doi.org/10.1061/(ASCE)GT.1943-5606.0001608)
17. Almohana A., Richards D.J., Stringfellow A.M.: The geotechnical properties of high organic content waste, Sardinia 2017, 16th International waste management and landfill symposium, S. Margherita di Pula (CA), Italy, 2–6 October (2017)
18. Chen, Y.M., Zhan, T.L.T., Wei, H.Y., Ke, H.: Aging and compressibility of municipal solid wastes. *Waste Manage.* **29**, 86–95 (2009)
19. Chen, Y., Ke, H., Fredlund, D.G., Zhan, L., Xie, Y.: Secondary compression of municipal solid wastes and a compression model for predicting settlement of municipal solid waste landfills. *J. Geotech. Geoenviron. Eng.* **136**(5), 706–717 (2010)


20. Hadinata, F., Damanhuri, E., Rahardyan, B., Widyarsana, I.M.W.: Identification of initial settlement of municipal solid waste layers in Indonesian landfill. *Waste Manage. Res.* **36**(8), 737–743 (2018)
21. Thakur, D., Gupta, A.K., Ganguly, R.: Geotechnical properties of fresh and degraded MSW in the foothill of Shivalik Range Una, Himachal Pradesh. *Int. J. Recent Technol. Eng.* (2019). <https://doi.org/10.35940/ijrte.B1497.078219>
22. Zeng, G., Ma, J., Hu, D., Wang, J.: Experimental study on compression and intrinsic permeability characteristics of municipal solid waste. *Adv. Civ. Eng.* (2019). <https://doi.org/10.1155/2019/3541635>
23. Bidlingmaier, W., Scheelhaase, T., Maile, A.: Langzeitverhalten von mechanisch-biologisch vorbehandeltem Restmüll auf der Deponie, Abschlußbericht zum Teilvorhaben 3.1 des BMBF-Verbundvorhabens "Mechanisch-biologische Behandlung von zu deponierenden Abfällen Universität Gesamthochschule Essen, Fachbereich 10 – Bauwesen, Fachgebiet Abfallwirtschaft (1999)
24. Duellmann, H.: Untersuchungen zum Einbau von MBA-Abfällen auf der Zentraldeponie Hannover, Laboruntersuchungen zum Verdichtungs-, Durchlässigkeits-, Last-Setzungs- und Scherverhalten. Februar 2002. Im Auftrag des Abfallwirtschaftsbetriebes Hannover (2002)
25. Carrubba, P., Cossu, R.: Investigation on compressibility and permeability of pre-treated waste mixture. In: Christensen, T.H., Cossu, R., Stegmann, R. (eds) Proceedings of the 9th international waste management and landfill symposium, S. Margherita di Pula, 6–10 October, Cagliari, Sardinia, Italy (2003)
26. Heiss-Ziegler, C., Fehrer, K.: Geotechnical behaviour of mechanically-biologically pretreated MSW. In: Proceedings Sardinia 2003, 9th International Waste Management and Landfill Symposium S. Margherita di Pula, Cagliari, Italy, 6–10 October (2003)
27. Bauer, J., Münnich, K., Fricke, K.: Investigation of Mechanical Properties of MBT Waste. In: Proceedings of the Fourth Asian-Pacific Landfill Symposium, Shanghai, China (2006)
28. Münnich, K., Bauer, J., Bahr T., Fricke K.: Landfilling of pre-treated waste - consequences for the construction and operation of landfills, Conference "The future of residual waste management in Europe" (2005)
29. Velkushanova, K.: Characterization of wastes towards sustainable landfilling by some physical and mechanical properties with an emphasis on solid particles compressibility, PhD Thesis, Faculty of Engineering and the Environment, University of Southampton (2011)
30. Hyun Il, P., Borinara, P., Hong, K.D.: Geotechnical considerations for end-use of old municipal solid waste landfills. *Int. J. Environ. Res.* **5**(3), 573–584 (2011)
31. Siddiqui, A.A., Richards, D.J., Powrie, W.: Investigations into the landfill behaviour of pretreated wastes. *Waste Manage.* **32**, 1420–1426 (2012). <https://doi.org/10.1016/j.wasman.2012.03.016>
32. Zordan J., Gourc J. P., Oxarango I., Conte M., Carrubba P.: Biomechanical behaviour of MSW: settlements-biodegradation relationship study through experiment and modelling. In: Proceedings of Sardinia 2013, 14th International Waste Management and Landfill Symposium, S. Margherita di Pula, 30 September - 4 October, Cagliari, Sardinia, Italy (2013).
33. Bortoluzzi, A.: Behaviour of an MBT waste in monotonic triaxial shear test, PhD thesis, University of Padova, Department of Civil Engineering (2014)
34. Petrovic, I., Stuhec, D., Kovacic, D.: Large oedometer for measuring stiffness of MBT waste. *Geotech. Test. J.* **37**(2), 296–310 (2014). <https://doi.org/10.1520/GTJ20130015>
35. Lakshmiathan, P., Santhosh, L.G., Sivakumar Babu, G.L.: Evaluation of the mechanical and hydrological characteristics of a bioreactor landfill using laboratory simulators, digital proceeding of ICOCEE – Cappadocia (2015)
36. Zhang, Z., Fang, Y., Wang, Y., Xu, H.: Compression behaviors of mechanically biologically treated wastes of Tianziling landfill in Hangzhou, China. *Environ. Sci. Pollut. Res.* **27**, 43970–43986 (2020). <https://doi.org/10.1007/s11356-020-10253-w>
37. Kuehle-Weidemeier, M.: Landfilling and properties of MBP waste, Proceedings Sardinia 2003. In: 9th International Waste Management and Landfill Symposium, S. Margherita di Pula, Cagliari, 6–10 October (2003)
38. Ziehm, G.: Verändern des mechanischen Verhaltens durch die mechanische und biologische Vorbehandlung, Deponierung von vorbehandelten Siedlungsabfällen. Veröffentlichungen des Zentrums fuer Abfallforschung der Technischen Universität Braunschweig, Heft **14**, 1–9 (1999)
39. Navaee-Ardeh, S., Bertrand, F., Stuart, P.R.: Development and Experimental evaluation of a 1D distributed model of transport phenomena in a continuous biodrying process for pulp and paper mixed sludge. *Dry. Technol.* **29**(2), 135–152 (2011). <https://doi.org/10.1080/07373937.2010.482723>
40. Tambone, F., Scaglia, B., Scotti, S., Adani, F.: Effects of biodrying process on municipal solid waste properties. *Bioresour. Technol.* **102**, 7443–7450 (2011). <https://doi.org/10.1016/j.biortech.2011.05.010>
41. Yang, B., Zhang, L., Jahng, D.: Importance of initial moisture content and bulking agent for biodrying sewage sludge. *Dry. Technol.* **32**(2), 135–144 (2013). <https://doi.org/10.1080/07373937.2013.795586>
42. Dominczyk, A., Krzystek, L., Ledakowicz, S.: Biodrying of organic municipal wastes and residues from the pulp and paper industry. *Dry. Technol.* **32**(11), 1297–1303 (2014). <https://doi.org/10.1080/07373937.2014.901349>
43. Yang, B., Hao, Z., Jahng, D.: Advances in biodrying technologies for converting organic wastes into solid fuel. *Dry. Technol.* **35**(16), 1950–1969 (2017). <https://doi.org/10.1080/07373937.2017.1322100>
44. Slezak, R., Krzystek, L., Ledakowicz, S.: Biological drying of municipal solid waste from landfill. *Dry. Technol.* **38**(1–2), 189–199 (2019). <https://doi.org/10.1080/07373937.2019.1611599>
45. Ham, G.Y., Matsuto, T., Tojo, Y., Matsuo, T.: Material and moisture balance in a full-scale bio-drying MBT system for solid recovered fuel production. *J. Mater. Cycles Waste Manage.* **22**, 167–175 (2019). <https://doi.org/10.1007/s10163-019-00925-2>
46. Ham, G.Y., Lee, D.H., Matsuto, T., Tojo, Y., Park, J.R.: Simultaneous effects of airflow and temperature increase on water removal in bio-drying. *J. Mater. Cycles Waste Manage.* **22**, 1056–1066 (2020). <https://doi.org/10.1007/s10163-020-01000-x>
47. Terzaghi, K.: The shearing resistance of saturated soils and the angle between the planes of shear. In: 1st International Conference on Soil Mechanics and Foundation Engineering, pp. 54–56 (1936)
48. Shariatmadari, et al.: Municipal solid waste effective stress analysis. *Waste Manage.* **29**, 2918–2930 (2009)
49. Biot, M.A.: General theory of three-dimensional consolidation. *J. Appl. Phys.* **12**, 155–164 (1941)
50. Skempton, A.W.: Effective stress in soils, concrete and rocks. In: Proc. Conf. Pore Pressure and Suction in Soils (1961)
51. de Boer, T.: Highlights in the historical development of the porous media theory: toward a consistent macroscopic theory. *Appl. Mech. Rev.* **49**, 201–262 (1996)
52. Ehlers, W.: Effective stresses in multiphase porous media: a thermodynamic investigation of a fully non-linear model with compressible and incompressible constituents. *Geomech. Energy Environ.* **15**, 35–46 (2018). <https://doi.org/10.1016/j.gete.2017.11.004>
53. Zhang, Z., Wang, Y., Hui, Xu., Fang, Y., Dazhi, Wu.: Influence of effective stress and dry density on the permeability of municipal solid waste. *Waste Mang. Res.* (2018). <https://doi.org/10.1177/0734242X18763520>

54. Powrie, W., Xu, X.-B., Richards, D., Zhan, L.-T., Chen, Y.-M.: Mechanisms of settlement in municipal solid waste landfills. *Journal of Zhejiang University-SCIENCE A (Applied Physics & Engineering)*, ISSN 1673–565X (Print); ISSN 1862–1775 (Online) (2019)
55. Liang, J.Y., Li, Y.M., Bauer, E.: A macro-microscopic coupled constitutive model for fluid-saturated porous media with compressible constituents. *Transp. Porous Media* (2022). <https://doi.org/10.1007/s11242-021-01725-9>
56. Sowers, G.F.: Settlement of waste disposal fills. *Proceedings of the 8th International Conference on Soil Mechanics and Foundation Engineering*, pp. 207–210 (1973)
57. Brauns, J., Kast, K., Blinde, A.: Compaction effects on the mechanical and saturation behaviour of disintegrated rockfill. *Proc. Int. Conf. Compact*, 1, 107–112 (1980)
58. Bauer, E.: Hypoplastic modelling of moisture-sensitive weathered rockfill materials. *Acta Geotech.* **4**, 261–272 (2009)
59. Ham, T.G., Nakata, Y., Orense, R., et al.: Influence of water on the compressive behavior of decomposed granite soil. *J. Geotech. Geoenviron. Eng.* **136**(5), 697–705 (2010)
60. Bauer, E., Fu, Z., Liu, S.: Influence of pressure and density on the rheological properties of rockfills. *Front. Struct. Civ. Eng.* **6**, 25–34 (2012). <https://doi.org/10.1007/s11709-012-0143-0>
61. Bareither, C.A., Benson, C.H., Edil, T.B.: Compression of municipal solid waste in bioreactor landfills: mechanical creep and biocompression. *J. Geotech. Geoenviron. Eng.* **2013**(139), 1007–1021 (2013)
62. Siddiqui, A.A., Powrie, W., Richards, D.J.: Settlement characteristics of mechanically biologically treated wastes. *J. Geotech. Geoenviron. Eng.* **139**(10), 1676–1689 (2013)
63. Landva, A.O., Valsangkar, A.J., Pelkey, S.G.: Lateral Earth Pressure at rest and compressibility of municipal solid waste. *Can. Geotech. J.* **37**, 1157–1165 (2000)
64. Hossain S.M., Gabr M.A.: Prediction of municipal solid waste landfill settlement with leachate recirculation. *Proceedings of the Geo-Frontiers Congress 2005*, ASCE, 168, 50. Austin, Texas (2005)
65. Singh, M.K.: Characterization of stress-deformation behaviour of municipal solid waste. PhD thesis. University of Saskatchewan, Saskatoon, SK, p. 292 (2008).
66. Rakic, D., Caki, L., Hadzi-Nikovic, G., Basaric, I.: Compressibility parameters of old municipal waste from two landfills in Serbia. *Proceedings of the XVI ECSMGE Geotechnical Engineering for Infrastructure and Development*, pp. 2741–2746 (2015). <https://doi.org/10.1680/ecsmge.60678>
67. Handy, R.L.: First-order rate equations in geotechnical engineering. *J. Geotech. Geoenviron. Eng.* **128**, 416–425 (2002). [https://doi.org/10.1061/\(ASCE\)1090-0241\(2002\)128:5\(416\)](https://doi.org/10.1061/(ASCE)1090-0241(2002)128:5(416))
68. Petrovic, I., Kaniski, N., Hrnčić, N., Bosilj, D.: Variability in the solid particle density and its influence on the corresponding void ratio and dry density: a case study conducted on the MBT reject waste stream from the MBT plant in Marišćina, Croatia. *Appl. Sci.* **12**(12), 6136 (2022). <https://doi.org/10.3390/app12126136>
69. ASTM International: Standard Guide for Laboratory Subsampling of Media Related to Waste Management Activities (D6323–19). ASTM International, West Conshohocken, PA (2019)
70. ASTM International: Standard Test Method for Particle-size Analysis of Soils (Withdrawn 2016) (D422–63). ASTM International, West Conshohocken, PA (2007)
71. ASTM International: Standard Test Methods for Determining the Water (Moisture) Content, Ash Content, And Organic Material of Peat and Other Organic Soilss (D2974–20e1). ASTM International, West Conshohocken, PA (2020)
72. ASTM International: Standard Test Method for Specific Gravity of Soil Solids by Gas Pycnometer, (D 5550–14). ASTM International, West Conshohocken, PA (2016)
73. Yesiller, N., Hanson, J.L., Cox, J.T., Noce, D.E.: Determination of specific gravity of municipal solid waste. *Waste Manage.* **34**(5), 848–858 (2014)
74. Brauns, J., Kast, K., Blinde, A.: Compaction effects on the mechanical and saturation behavior of disintegrated rockfill. *Proc. Int. Conf.* **1**, 107–112 (1980)
75. Ovalle, C., Dano, C., Hicher, P.Y., Cisternas, M.: Experimental framework for evaluating the mechanical behavior of dry and wet crushable granular materials based on the particle breakage ratio. *Can. Geotech. J.* **52**, 587–598 (2015)
76. Bauer, E.: Constitutive modelling of wetting deformation of rockfill materials. *Int. J. Civ. Eng.* **17**, 481–486 (2019)
77. Ohde, J.: Zur Theorie der Druckverteilung im Baugrund. *Bauingenieur* **20**, 451–459 (1939). ((in German))
78. Janbu, N.: Soil compressibility as determined by oedometer and triaxial tests. *Proceedings of European Conference on Soil Mechanics and Foundation Engineering (ECSMFE)*, Wiesbaden, Vol. 1, pp. 19–25 (1963) (in German).
79. Bauer, E.: Zum mechanischen Verhalten granularer Stoffe unter vorwiegend ödometrischer Beanspruchung, p. 130. *Veröffentlichungen des Institutes für Boden- und Felsmechanik der Universität Karlsruhe*, Heft (1992). (in German)
80. Reddy, K.R., Hettiarachchi, H., Gangathulasi, J., Bogner, J.E.: Geotechnical properties of municipal solid waste at different phases of biodegradation. *Waste Manage.* **31**, 2275–2286 (2011)

Publisher's Note Springer Nature remains neutral with regard to jurisdictional claims in published maps and institutional affiliations.

Springer Nature or its licensor (e.g. a society or other partner) holds exclusive rights to this article under a publishing agreement with the author(s) or other rightsholder(s); author self-archiving of the accepted manuscript version of this article is solely governed by the terms of such publishing agreement and applicable law.

Authors and Affiliations

Nikola Kaniški¹ · Nikola Hrnčić¹ · Igor Petrović¹  · Erich Bauer²

✉ Igor Petrović
igor.petrovic@gfv.unizg.hr

² Institute of Applied Mechanics, Graz University of Technology, Technikerstrasse 4, 8010 Graz, Austria

¹ Faculty of Geotechnical Engineering, University of Zagreb, Hallerova Aleja 7, 42000 Varaždin, Croatia